STRUCTURAL ANALYSIS AND PHOTOLUMINESCENCE PROPERTIES OF Er^{3+} DOPED $SrBi_2Nb_2O_9$ FERROELECTRIC CERAMIC

A DISSERTATION

SUBMITTED IN PARTIAL FULFILLMENT OF THE REQUIREMENTS FOR THE AWARD OF THE DEGREE OF

MASTER OF SCIENCE
IN
PHYSICS

Submitted by:
RITUSHREE SHAILY
(2K19/MSCPHY/23)
and
POOJA MOJUMDAR
(2K19/MSCPHY/19)

Under the supervision of:
DR. RENUKA BOKOLIA

DEPARTMENT OF APPLIED PHYSICS
DELHI TECHNOLOGICAL UNIVERSITY
(Formerly Delhi College of Engineering)
Bawana Road, Delhi-110042

MAY, 2021

DEPARTMENT OF APPLIED PHYSICS
DELHI TECHNOLOGICAL UNIVERSITY
(Formerly Delhi College of Engineering)
Bawana Road, Delhi-110042

CANDIDATE'S DECLARATION

We, ***Ritushree Shaily (2K19/MSCPHY/23)*** *and* ***Pooja Mojumdar (2K19/MSCPHY/19)*** students of M.Sc. Physics, hereby declare that the project Dissertation titled ***"Structural analysis and photoluminescence properties of Er^{3+} doped $SrBi_2Nb_2O_9$ ferroelectric ceramic"*** which is submitted by us to the Department of Applied Physics, Delhi Technological University, Delhi in partial fulfillment of the requirement for the award of the degree of Master of Science, is original and not copied from any source without proper citation. This work has not previously formed the basis for the award of any Degree, Diploma Associateship, Fellowship or other similar title or recognition.

Place: Delhi
Date: 31.05.2021

RITUSHREE SHAILY

POOJA MOJUMDAR

DEPARTMENT OF APPLIED PHYSICS
DELHI TECHNOLOGICAL UNIVERSITY
(Formerly Delhi College of Engineering)
Bawana Road, Delhi-110042

CERTIFICATE

I hereby certify that the Project Dissertation titled ***"Structural and photoluminescence properties of Er^{3+} doped $SrBi_2Nb_2O_9$ ceramics"*** which is submitted by ***Ritushree Shaily and Pooja Mojumdar***, roll nos. ***2K19/MSCPHY/23*** and ***2K19/MSCPHY/19***, Department of Applied Physics, Delhi Technological University, Delhi in partial fulfillment of the requirement for the award of the degree of Master of Science, is a record of the project work carried out by the students under my supervision. To the best of my knowledge this work has not been submitted in part or full for any Degree or Diploma to this University or elsewhere.

Renuka

Place: Delhi
Date: 31.05.2021

Dr. RENUKA BOKOLIA
SUPERVISOR

PLAGIARISM REPORT

Pooja

turnitin

Final Report 1.docx
May 31, 2021
4350 words / 24551 characters

Renuka

Final Report 1.docx

31.05.2021

Sources Overview

6%
OVERALL SIMILARITY

1	l03.iphy.ac.cn INTERNET	<1%
2	FAN, S.. "Ferroelectric properties of sol-gel derived Nd-doped SrBi"4Ti"4O"1"5 thin films", Journal of Rare Earths, 200808 CROSSREF	<1%
3	ajer.org INTERNET	<1%
4	static.horiba.com INTERNET	<1%
5	Rasu Manimuthu, Thaneswari, Krithikadevi Ramachandran, Abimanyu Sugumaran, Siva Chidambaram, Arulmozhi Muthukumarasamy, and Balraj Baskaran. "Cytotoxic potentials o... CROSSREF	<1%
6	University of Sheffield on 2017-08-22 SUBMITTED WORKS	<1%
7	espace.curtin.edu.au INTERNET	<1%
8	Jawaharlal Nehru University (JNU) on 2017-06-15 SUBMITTED WORKS	<1%
9	John-Christopher Boyer, Louis A. Cuccia, John A. Capobianco. " Synthesis of Colloidal Upconverting NaYF : Er /Yb and Tm /Yb Monodisperse Nanocrystals ", Nano Letters, 2007 CROSSREF	<1%
10	Rajni Jain. "Piezoelectric properties of nonstoichiometric Sr[sub 1−x]Bi[sub 2+2x/3]Ta[sub 2]O[sub 9] ceramics", Journal of Applied Physics, 2005 CROSSREF	<1%
11	file.scirp.org INTERNET	<1%
12	profdoc.um.ac.ir INTERNET	<1%
13	Kwame Nkrumah University of Science and Technology on 2013-02-22 SUBMITTED WORKS	<1%
14	Visvesvaraya National Institute of Technology on 2019-12-23 SUBMITTED WORKS	<1%
15	Sameer Jain, Prasun Ganguly, Sheela Devi, A. K. Jha. " Structural, Dielectric and Ferroelectric Studies of Molybdenum Substituted Sr Bi Nb O Ferroelectric Ceramics ", Ferroelectric... CROSSREF	<1%
16	Xiao, H.D.. "Synthesis and structural properties of GaN particles from GaO"2H powders", Diamond & Related Materials, 200510 CROSSREF	<1%
17	Zhihang Peng, Dongxu Yan, Qiang Chen, Deqiong Xin, Dan Liu, Dingquan Xiao, Jianguo Zhu. "Crystal structure, dielectric and piezoelectric properties of Ta/W codoped Bi3TiNbO9 ... CROSSREF	<1%
18	creativecommons.org INTERNET	<1%

Excluded search repositories:
- None

Excluded from Similarity Report:
- Bibliography
- Quotes
- Small Matches (less than 10 words).

Excluded sources:
- None

ACCEPTANCE RECORD

Department of Mechanical Engineering, CMRIT, Bengaluru, India &
Core-Facility Centre for Photochemistry and Nanomaterials, GNU, South Korea

Certificate of Presentation

Paper ID: MATPR-D-21-03789

This is to certify that

Prof./Dr./Mr./Ms ***Ms.Pooja Mojumdar***

From

Delhi Technological University, Delhi

has presented the paper titled

Structural Properties Of Strontium Bismuth Niobate(SrBi2Nb2O9) Ferroelectric Ceramics

Authored by

Ms.Pooja Mojumdar, Ms.Ritushree Shaily, Dr.Renuka Bokolia

at

International Conference on Futuristic Research in Engineering Smart Materials

FRESM '21

held Online on 23rd and 24th of April, 2021

Dr. Arunkumar T	**Dr. Ramachandran S**	**Dr. Myong Yong Choi**	**Dr. Sanjay Jain**
Organizing Secretary	Convener	Convener	Principal, CMRIT

ELSEVIER

Track Your Accepted Article

The easiest way to check the publication status of your accepted article

Structural properties of Strontium Bismuth Niobate (SrBi2Nb2O9) Ferroelectric Ceramics

Article reference	MATPR25695
Journal	Materials Today: Proceedings
Corresponding author	Renuka Bokolia
First author	Pooja Mojumdar
Received at Editorial Office	31 Mar 2021
Article revised	22 May 2021
Article accepted for publication	24 May 2021

ISSN 2214-7853

Last update: 31 May 2021

Share via email

Department of Mechanical Engineering, CMRIT, Bengaluru, India &
Core-Facility Centre for Photochemistry and Nanomaterials, GNU, South Korea

Certificate of Presentation

Paper ID: MATPR-D-21-03797

This is to certify that

Prof./Dr./Mr./Ms ***Ms. Ritushree Shaily***

From

Delhi Technological University

has presented the paper titled

Structural And Photoluminescence Properties Of Er3+ Doped SrBi2Nb2O9 Ceramics

Authored by

Ms. Ritushree Shaily, Dr. Renuka Bokolia

at

International Conference on Futuristic Research in Engineering Smart Materials

FRESM '21

held Online on 23rd and 24th of April, 2021

Sanjy

ELSEVIER

Track Your Accepted Article

The easiest way to check the publication status of your accepted article

Structural and photoluminescence properties of Er3+ doped SrBi2Nb2O9 ceramics

Article reference	MATPR25693
Journal	Materials Today: Proceedings
Corresponding author	Renuka Bokolia
First author	Ritushree Shaily
Received at Editorial Office	31 Mar 2021
Article revised	23 May 2021
Article accepted for publication	24 May 2021

ISSN 2214-7853

Last update: 31 May 2021

Share via email

REGISTRATION RECORD

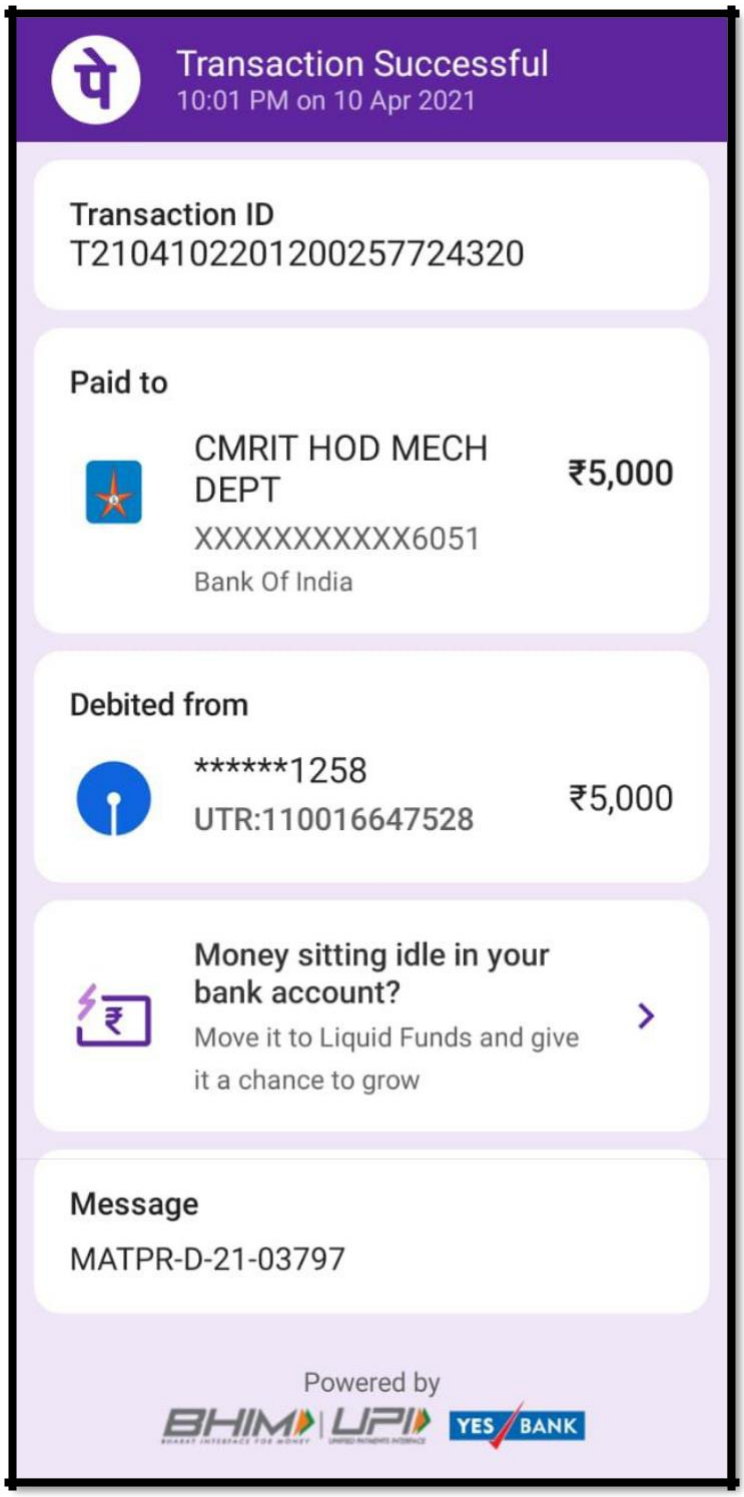

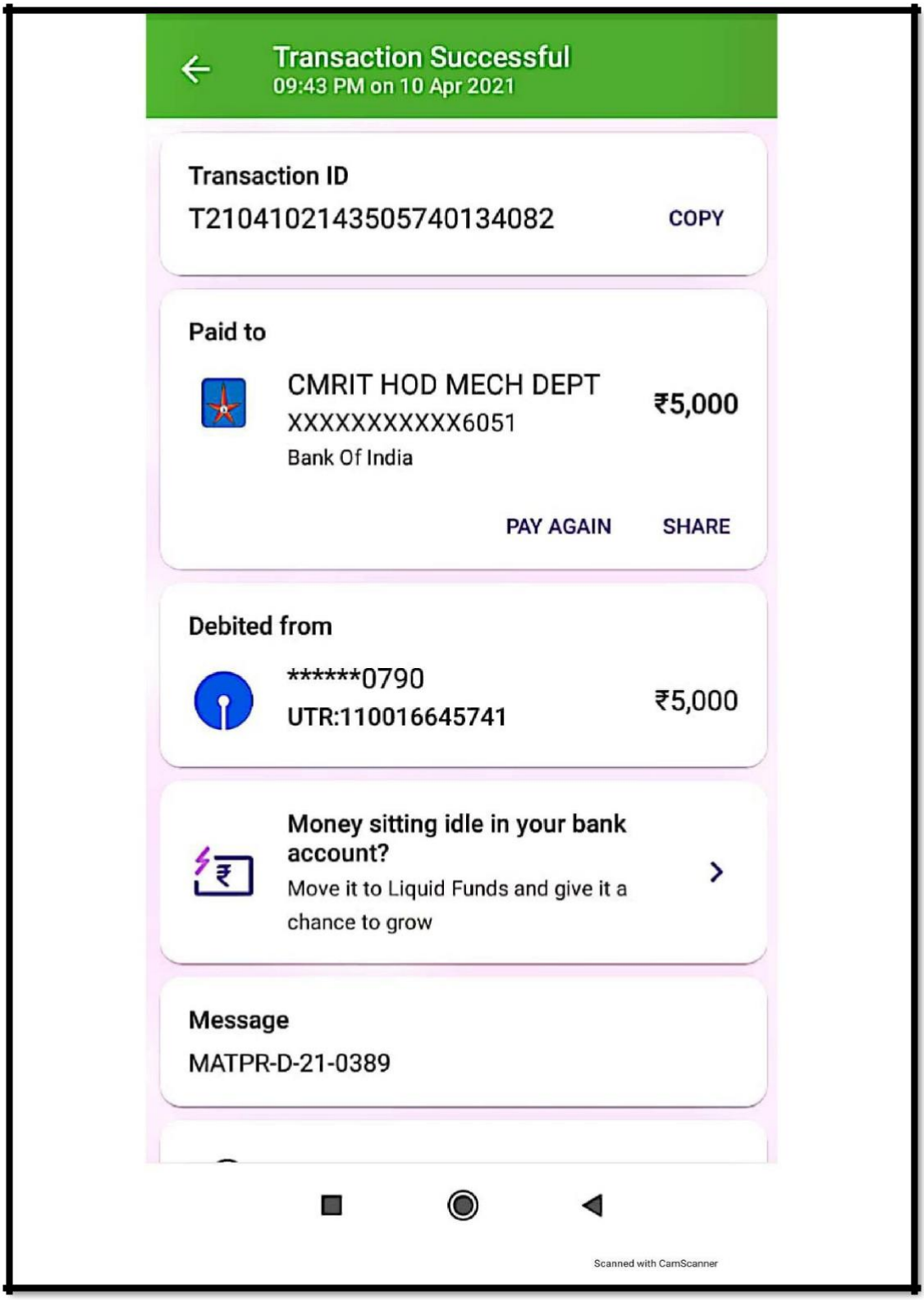
Transaction Successful
09:43 PM on 10 Apr 2021
Transaction ID
T210410214350574013408 2
COPY
Paid to
CMRIT HOD MECH DEPT
XXXXXXXXXXX6051
Bank Of India
₹5,000
PAY AGAIN
SHARE
Debited from
******0790
UTR:110016645741
₹5,000
Money sitting idle in your bank account?
Move it to Liquid Funds and give it a chance to grow
Message
MATPR-D-21-0389
Scanned with CamScanner

ACKNOWLEDGEMENT

We would like to express our sincere gratitude and deep appreciation to our esteemed guide ***Dr. Renuka Bokolia***, Assistant Professor, Delhi Technological University (DTU), for her invaluable support and guidance and for having faith in us that we can deal with this project.

We would like to extend our deepest gratitude to ***Miss Ankita Banwal***, Research Scholar, DTU, for helping us through thick and thin while performing experiments, for beginners like us which was not easy, also for her invaluable discussions on several topics that provided a good understanding of the topics. We wish her all the best in her future endeavours.

We would also like to thank our parents, for their constant mental support.

RITUSHREE SHAILY

POOJA MOJUMDAR

ABSTRACT

The polycrystalline $SrBi_2Nb_2O_9$ (SBN) and Er^{3+} doped $SrBi_{2-x}Nb_2Er_xO_9$ (x = 0.00, 0.01, 0.02, 0.03, 0.04, 0.05) ceramics at these different concentrations were synthesized by conventional solid-state method. The pure SBN underwent heat treatment at different calcination temperatures: 800ºC, 850ºC, and 950ºC, and the evolution of phases were studied at these different calcination temperatures. At 950ºC, no traces of secondary phases were seen in pure SBN thus Er^{3+} doped $SrBi_{2-x}Nb_2Er_xO_9$ at different concentrations were calcined at this temperature followed by sintering of all the samples at 1000ºC of temperature. Few secondary phases have been identified along with the desired SBN phase but begin to decrease with the increase in the calcination temperature. confirms the formation of single-phase material with orthorhombic structure. From XRD analysis of pure and Er^{3+} doped $SrBi_{2-x}Nb_2Er_xO_9$ (x = 0.00, 0.01, 0.02, 0.03, 0.04, 0.05) with an increasing content of Erbium (Er^{3+}), an increase in the lattice parameters and unit cell volume was observed. The structural morphology of pure and Er^{3+} doped SBN, sintered at 1000ºC were investigated under SEM revelled the formation of the highly dense grains with more pores and non-uniform grain size and EDS provides information about the elemental composition. The Raman analysis revealed the formation of the orthorhombic phase of pure SBN. The photoluminescence properties for Er^{3+} doped $SrBi_{2-x}Nb_2Er_xO_9$ (x = 0.00, 0.01, 0.02, 0.03, 0.04, 0.05) at different concentrations were also investigated. Strong green emission at 549.8 nm was seen at an excitation wavelength, λex = 480 nm at room temperature for an Er content (x = 0.03), attributed to $^4S3/2 \rightarrow {}^4I15/2$ transitions.

CONTENTS

I. LIST OF FIGURES

II. LIST OF TABLES

III. LIST OF SYMBOLS

BLSF	: Bismuth Layered Structure Ferroelectric
SBN	: Strontium Bismuth Niobate
℃	: Degree of Celsius
wt.	: Weight
λ	: Wavelength
θ	: Angle of diffraction
D	: Average crystalline size
β	: Full width at half maximum
FWHM	: Full width at half maximum
JCPDF	: Joint committee on powder diffraction standards
a, b, c	: Lattice parameters
PVA	: Polyvinyl alcohol
XRD	: X-Ray Diffraction
SEM	: Scanning electron microscope
EDS	: Energy Dispersive Spectroscopy
PL	: Photoluminescence

Chapter 1:

Introduction

Ferroelectric materials, a type of materials that hold spontaneous polarization and are reversible when subjected to an electric field. Recently, ferroelectric materials have drawn so much attention because of their excellent properties such as high dielectric constant, great fatigue resistance, high Curie temperature, and amazing piezoelectric effects making them attractive materials for different applications such as non-volatile random-access memories (NvRAM), optical switches and high capacitance capacitors etc. ***The bismuth layered structure ferroelectric (BLSFs) ceramics are ABO3-type perovskite piezoelectric materials.***

1.1 Structure:

The bismuth layered structure ferroelectric (BLSFs) ceramics, member of Aurivillius family with a chemical formula : $(Bi2O2)^{2+}$ $(Am\text{-}1BmO3m+1)^{2-}$, where A can be a mono-, di-, or trivalent element (or their combination) with coordination no. 12, for instance Ba^{2+}, Ca^{2+}, La^{3+}, Sm^{3+}, Bi^{3+}, Sr^{2+}, etc., furthermore B is a transition element suited to octahedral coordination possessing coordination no. 6 such as Fe^{3+}, Nb^{5+}, Ti^{3+}, Ta^{5+}, W^{6+},and Mo^{6+}, etc., and also, m denotes the number of perovskite layers intermediate between two bismuth oxide layers. Hereabouts, A could be Ca^{2+}, Pb^{2+}, Ba^{2+} and Sr^{2+}, etc. and B perhaps Ti $^{4+}$, Nb^{5+}, Ta^{5+}, V^{5+}, Mo^{5+}, and W^{6+} etc. Ferroelectric ceramics are very sensitive to compositional modifications such as by changing stoichiometry or even by doping ceramics with numerous elements notably modifying the ferroelectric properties and crystal structure of the ceramics. The value of ‘m’ lies between1 to 5. Currently, more than 70 compounds have been reported in this Aurivillius family and more than 50% of them are Ferroelectric. The schematic diagram for m=1 to 5 is shown in fig.1.

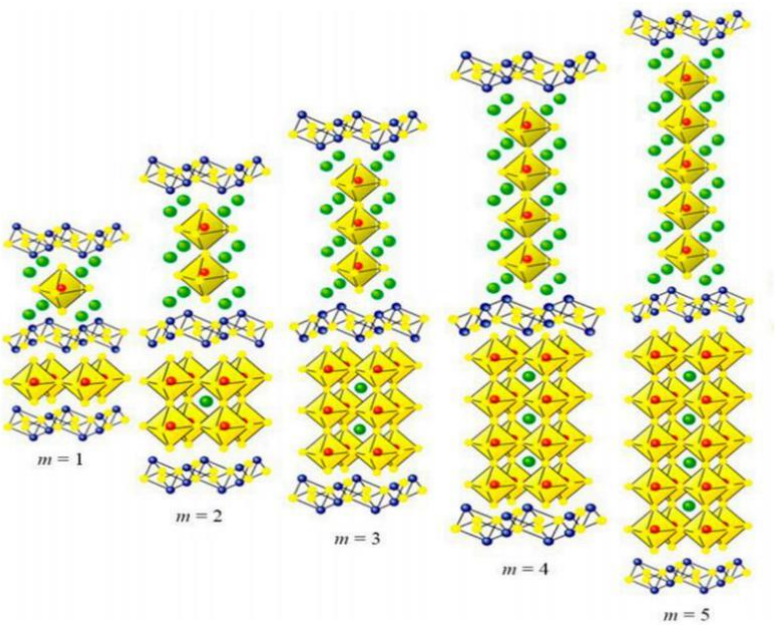

Fig.1. Aurivillius structure as a function of the number of the pseudo perovskite layer.

The perovskite $(Am\text{-}1BmO3m+1)^{2-}$ with octahedral layer m = 6,7 or 8 is difficult to synthesis and their existence is doubtful. The BSLF compound with an odd number of octahedra layer (m = 1,3,5) has crystal symmetry of B2cd space group. The compound with an even number of octahedral layers (m = 2,4) has crystal symmetry of A21am space group. For the even octahedra layer, the centre of the perovskite block falls in A-position and for the odd octahedra layer, pseudo-perovskite is in B-position. For this kind of structure, (Bi2O2) layer is parallel to the unit cell's ab plane (basal plane). The orthorhombic distortion can be seen in these structures where the c-parameter increases and both a and b decrease due to the presence of Bi^{3+} cations. This distortion can be decreased by replacing any symmetric cation with an asymmetric Bi^{3+} cation.

1.2 Types:

BSLF compound has been categorized into four parts:

1. $Bi_4Ti_3O_{13}$
2. Bi_3TiNO_9 (N= Nb, Ta)
3. $MBi_4Ti_4O_{15}$ (M= Ca, Sr, Ba, $K_{0.5}Bi_{0.5}$, $Na_{0.5}Bi_{0.5}$)
4. $MBi_2Nb_2O_9$

Among all these four types, $MBi_2Nb_2O_9$ family is most popular for research and application perspective. Main component of this family is $SrBi_2Nb_2O_9$ (SBN), $CaBi_2Nb_2O_9$ (CBN), $SrBi_2Ta_2O_9$ (SBT). Researchers on BSLF's are mainly working in preparation techniques and chemical composition for the last few years to enhance the quality of BSLF.

1.3 Properties:

BSLF has many properties such as high curie temperature, high dielectric constant, spontaneous polarization and, outstanding piezoelectric response. Bismuth layer-structured ferroelectrics (BLSF) have been studied tremendously in the form of thin-film because they are the best candidate for non-volatile ferroelectric random-access memory (FeRAM).

1.4 Organization of the Thesis:

This thesis is divided into five parts:

i. **Chapter 1** presents a brief introduction of BSLF and its structure.
ii. **Chapter 2** deals with the detailed study of one BSLF compound SBN($SrBi_2Nb_2O_9$). This section included the background information needed to understand the aim and objective of the investigation.
iii. **Chapter 3** explained the detailed experimental process related to research work.
iv. **Chapter 4** describes the result and discussion of characterization which have been done in the sample.
v. **Chapter 5** contains the conclusion.

Chapter 2:

Literature Review

2.1 Introduction

In this chapter, literature review on bismuth layer structure ferroelectric (BSLF) ceramic, $SrBi_2Nb_2O_9$(SBN) has been done with respect to synthesis method and structure-property. The study of phase evolution at different temperatures, morphology, and the effect of ionic substitution on the structure and on the optical property have been studied. The review has been done on $SrBi_2Nb_2O_9$.

2.2 Strontium Bismuth Niobate (SBN)

The chemical formula of SBN is $SrBi_2Nb_2O_9$, lead-free ferroelectric member of Bismuth Layered Structure Ferroelectric Ceramics belonging to the Aurivillius family (n = 2) has drawn consideration on account of their remarkable characteristics such as a high Curie temperature, Tc (~718K), great fatigue resistance, low dielectric loss, reasonable spontaneous polarization, and temperature-insensitive high piezoelectric coefficient and considered for high-temperature applications. $SrBi_2Nb_2O_9$ (SBN) ceramic by conventional solid-state method and study the associated effect of doping of Er^{3+} on their respective crystal structures and luminescence properties. Pure SBN exist in orthorhombic phase, associated with the space group A21am. Some rare-earth ions like Er^{3+}, Eu^{3+}, Pr^{3+}, etc. are widely used as luminescence centres for their potential applications. Thus, by rare-earth doping, the electrical properties and strong luminescence of some ferroelectric materials gets enhanced.

2.3 Synthesis of BSLF

BSLF based compound synthesized by different methods such as conventional solid-state method, molten salt, mechanochemical activation route, hydrothermal method, self-propagating high-temperature synthesis, etc. However, the property of the final compound depends upon the characteristic of powder such as purity, particle size, Morphology. The final result of the material totally depends upon the purity of raw material and synthesis technique.

2.3 Solid-State reaction method

The solid-state synthesis can be done as firstly, all the desired highly purified raw samples were weighed in stoichiometric ratios and then were mixed together followed by grinding in mortar pestle. The obtained powder then undergoes heat treatment for a few hours. The calcination of obtained powder results in the decomposition of the starting reagents and removes the volatile products such as NH3, NO2, CO2, and H2O, only remain the oxides.

Followed by the sintering of samples just to make sure that no secondary phases were present in the required samples.

Flow chart of Solid-state reaction method

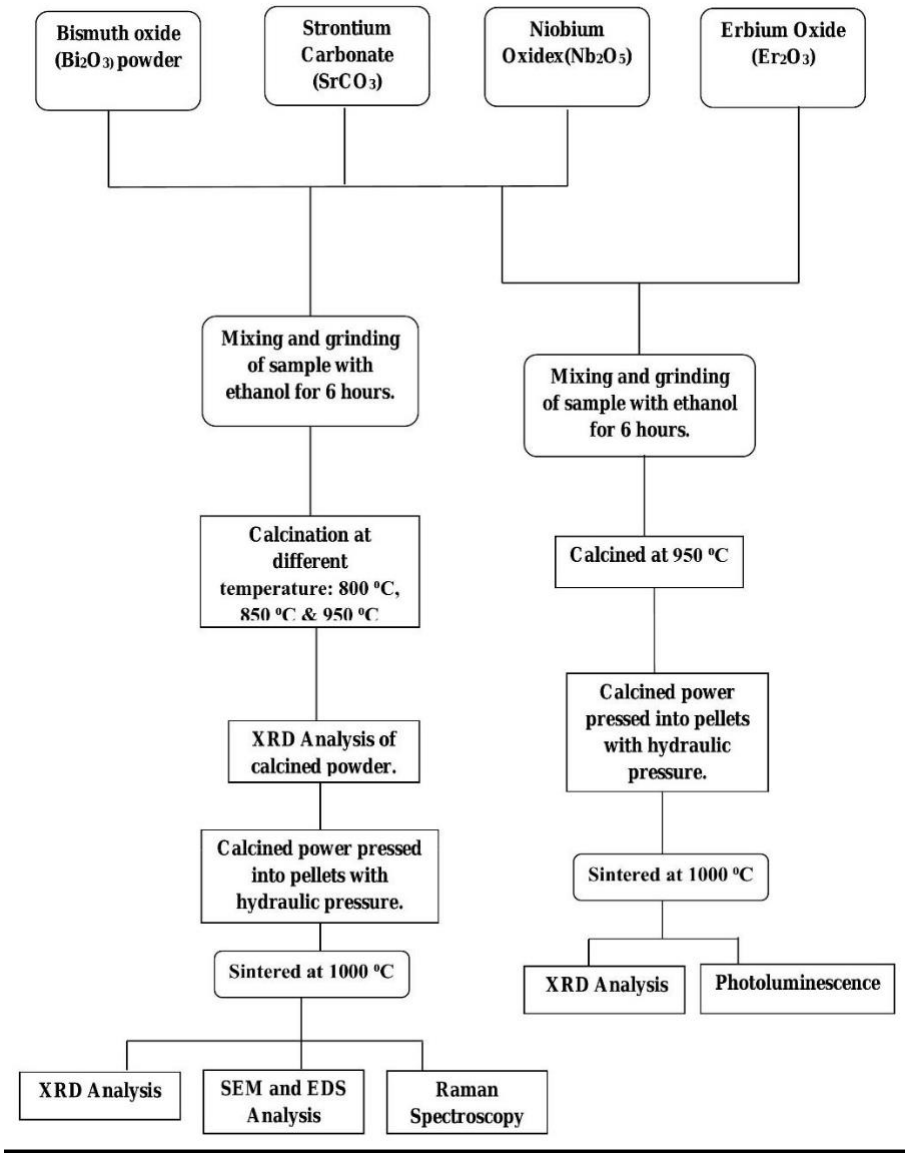

2.4 Objective of the work

I. To study variations in phase evolution at different calcination temperatures during the preparation of $SrBi_2Nb_2O_9$ ceramic to get a single-phase SBN with no impurity phase.

II. The synthesis of Er^{3+} doped $SrBi_2Nb_2O_9$(SBN) ceramic by conventional solid-state method and study the associated effect of doping of Er^{3+} on their respective crystal structures and luminescence properties.

Chapter 3:

Experimental work

3.1 Material Synthesis

In this experiment, the polycrystalline Er^{3+} doped SrBi2-*x*Nb2Er*x*O9 (*x* = 0.00, 0.01, 0.02, 0.03, 0.04, 0.05) ceramics in stoichiometric compositions were synthesized using conventional solid-state reaction method. Firstly, highly purified starting materials Nb2O5 (from Aldrich of 99.9% purity), SrCO3 (from Alfa Aesar of 97.5% purity), Bi2O3 (from Alfa Aesar of 97.5% purity), and Er2O3 (from Alfa Aesar of 97.5% purity) weighed in stoichiometric ratios and then these weighed samples were mixed. After that mixed sample was grinded into a mortar pestle with the addition of ethanol till it gets dried up and repeats the process for 6hours. Then the prepared samples were calcined at 950℃ for 7 hours. After calcination, 5 wt.% of polyvinyl alcohol (PVA), standard binder is added to the calcined samples and mixed rigorously and then disk-shaped green pellets of all samples were prepared with a diameter of 13 mm and thickness of 1mm by manual hydraulic press at a pressure of 50 MPa, and keep at rest for 1 min. Hereafter, green pellets of all samples were sintered at 1000℃ for 8 hours with intermediate heat treatment at 500℃ for 1hour in order to remove the binder from the pellets.

The equation for synthesis:

$$SrCO3 + Bi2O3 + Nb2O5 \rightarrow SrBi2Nb2O9 + CO2 \uparrow$$

3.2 Characterization Details

3.2.1 For XRD

The phase identification and analysis of crystal structure of Er^{3+} doped SrBi2-*x*Nb2Er*x*O9 (x = 0.00, 0.01, 0.02, 0.03, 0.04, 0.05) were done with the help of the X-Ray diffraction. The XRD spectra achieved by using the Bruker D-8 Advance X-ray diffractometer at Cu-Kα radiation (kα = 1.5406 Å). The XRD spectrum was observed within the range, $20^{o} \leq 2\theta \leq 70^{o}$. The peak of ceramics was matched with JCPDF file number 01-089-8154 to confirm the pure phase of SBN. The crystalline size has been calculated by Scherrer's equation:

$$D = \frac{0.89\,\lambda}{\beta cos\theta}$$

where, D is the average crystalline size, λ is Cu-Kα (λ =0.154nm) wavelength, β is the full width at half maximum (FWHM) of the diffraction peak, and θ is the angle of diffraction.

3.2.2 For SEM and EDS

The structural morphology and grain formation have been investigated on unpolished sintered ceramic pellets by using the JEOL 661 Scanning electron microscopy (SEM) equipped with Amkette energy dispersive spectrometer (EDS).

3.2.3 For Raman Spectroscopy

At room temperature, the Raman spectra were obtained by using the Horiba LabRam HR evolution spectrometer at wavelength 514 nm at 40 mW.

3.2.4 For Photoluminescence

The photoluminescence (PL) spectra of Er^{3+} doped SBN recorded at an excitation wavelength, $\lambda ex = 480$ nm.

Chapter 4:

Result and Discussion

4.1 X-Ray diffraction Analysis

Fig.1(a, b, c) depicts the evolution of phase that develops during the calcinations heat treatment at 800º C, 850º C, and 950º C of $SrBi_2Nb_2O_9$ (SBN) powder to form a single-phase of SBN. The calcination temperature uprises to 1000º C to ensure that single-phase SBN ($SrBi_2Nb_2O_9$) is formed. Highly pure raw materials $SrCO_3$, Nb_2O_5, and Bi2O3 were mixed stoichiometrically, as the reaction between them proceeds to lead to the formation of various intermediate phases accompanying the initial crystallization of $SrBi_2Nb_2O_9$ phase. During the reaction between Bi_2O_3 and Nb_2O_5 numerous phases e.g., $Bi_8Nb_{18}O_{57}$, $BiNbO_4$ and $Bi_5Nb_3O_{15}$ are formed. At 800°C calcined temperatures, the XRD pattern shows the presence of Bi_2O_3, $SrBi_2O_4$ (due to the reaction between Bi_2O_3 and $SrCO_3$), single-phase $Bi_5Nb_3O_{15}$, and some intermediate phase of $BiNbO_4$, existed side by side with desired single-phase $SrBi_2Nb_2O_9$ phase and the same intermediate phases were also detected at 850 °C. At 850º C, the XRD pattern shows the mix phase of $SrBi_2Nb_2O_9$ and Bi_2O_3 at 28.82º & 29.06º respectively. From the literature survey, we corresponding to Bi_2O_3 found that peaks phase seen at 2θ (31.66º, 47.08º, and 58.06º) because Bi2O3 remains unreacted but when it is treated to a higher range of temperature, the phase of Bi_2O_3 disappears. Also, it is interesting to see that intermediate phase i.e., $SrBi_2O_4$, $Bi_5Nb_3O_{15}$, and $BiNbO_4$ start decreasing with the increase in the calcination temperature. When the calcination temperature rises to 950°C no secondary phases are observed for the sample indicating that the reaction mechanism for the phase evolution of pure SBN is completed followed by sintering at 1000ºC. The peak of ceramics is matched with JCPDF file number 01-089-8154 confirms the pure SBN of single-phase and no secondary phases were detected. Thus, the reaction mechanism for obtaining the desire phase of $SrBi_2Nb_2O_9$, should be calcinated at 950ºC and sintered at 1000ºC. (Fig.2). The lattice parameters for pure SBN a = 5.4933 Å, b = 5.5136 Å, and c = 25.035 Å related to the orthorhombic phase, associated with the space group A21am. The lattice parameter was calculated with the help of PowderX software. Also, the highest diffraction peak associated with the (115) plane of $SrBi_2Nb_2O_9$ was detected. The average crystallite size of SBN was calculated by Scherrer's equation which is found to be 31.50nm. As the intensity and sharpness of the peak increases with an increase in temperature attributed to increase in crystallinity.

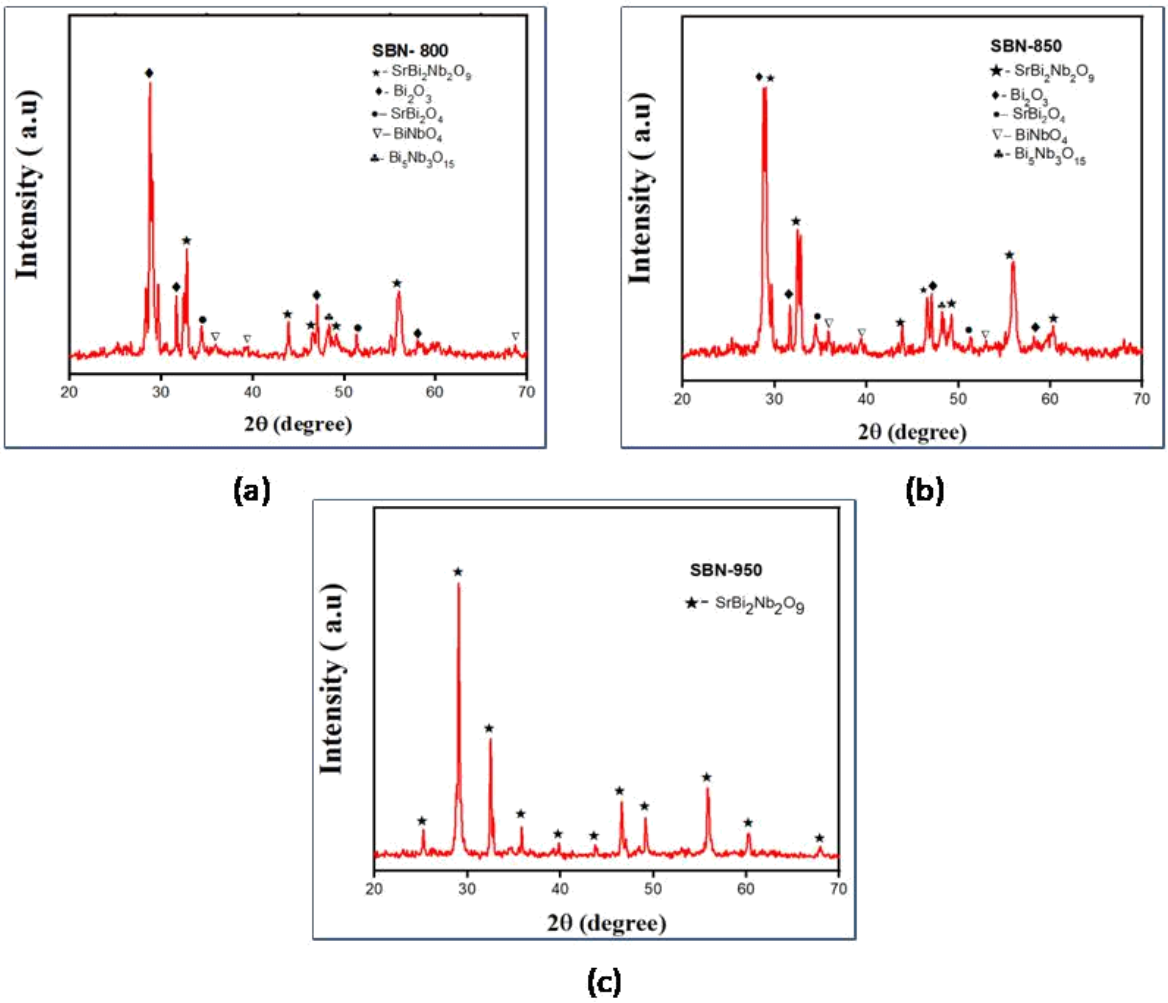

Fig.1. XRD pattern of $SrBi_2Nb_2O_9$ at different temperature (a) at 800° C (b).850° C (c) 950° C

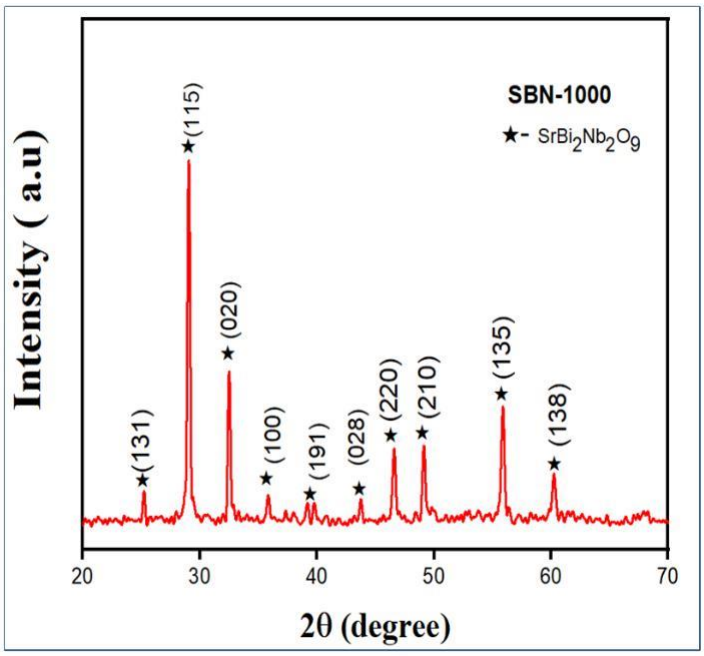

Fig.2. XRD pattern of powder $SrBi_2Nb_2O_9$ ceramic at sintering temperature 1000°C

As Erbium, rare earth metal belongs to the lanthanide series shows most stable +3 oxidation state thus it is easy to substitute Er^{+3} in a place of Bi^{+3}. Fig. 3, shows XRD spectra of pure $SrBi_2Nb_2O_9$ and Er^{3+} doped $SrBi_{2-x}Nb_2Er_xO_9$ ceramic powders at varying Er^{3+} concentrations (x = 0.00, 0.01, 0.02, 0.03, 0.04, 0.05). From the XRD analysis in the range $2\vartheta = 10^{\circ}$-80°, the observed Bragg's reflection was indexed and found closely matching with the standard diffraction pattern data of $SrBi_2Nb_2O_9$ with JCPDS card # 01-089- 8154 and confirmed the formation of single phase with no traces of secondary phases or unreacted phases present, specifying that Er^{3+} ions completely dissolved in SBN host lattice without any significant structural change of the host lattice. Thus, all samples crystallized in the orthorhombic phase, associated with the space group $A2_1am$. Also, the highest diffraction peak associated with (115) plane of $SrBi_2Nb_2O_9$ was detected for all concentrations conforming to the bismuth layered structure with n = 2 and the results are in agreement with the earlier reports indicating the strongest diffraction corresponding to (112n+1) reflection in the Aurivillius phase for BLSF compositions. The lattice parameters were calculated with the help of PowderX software, and the structural parameters tabulated in Table 1.

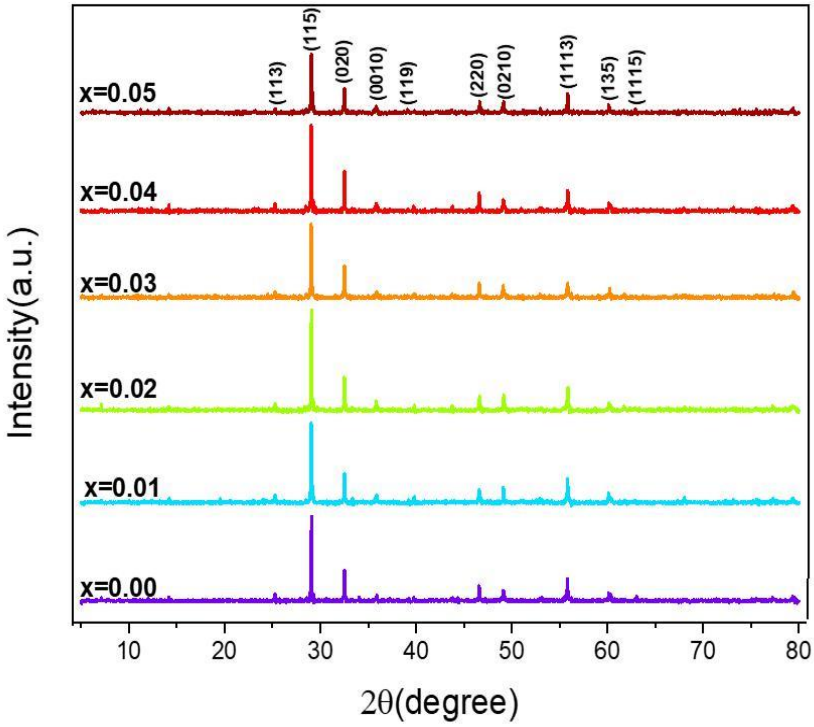

Fig.3 The XRD patterns of pure and Er^{3+} doped $SrBi_2Nb_2O_9$ at different concentrations of Er^{3+} based on the formula $SrBi_{2-x}Nb_2Er_xO_9$ ceramics.

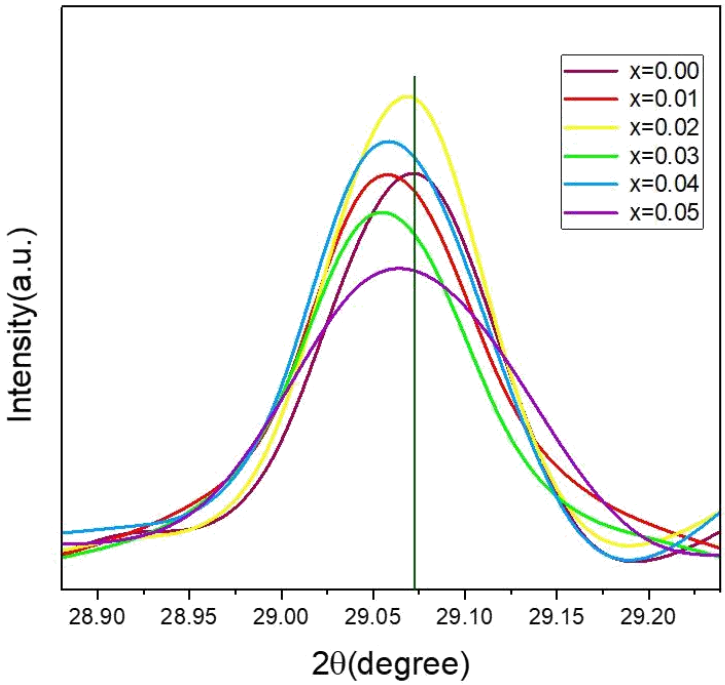

Fig.4. Shift of strongest XRD peaks (115) at different Erbium concentrations

It is noted from the Fig.4. with an increase in the concentration of Er^{3+} ions the XRD peaks at 29.08° shifted towards lower 2θ values shows that the Er^{3+} ions completely diffused into the host lattice along with the increase in lattice parameters which is due to the difference in ionic radii of Bi^{3+}(r = 102Å) and Er^{3+} (r = 0.88Å) leading to structural distortion and as seen through EDS compositional analysis in Table 3 the results are well supported with the increasing elemental ratio of (Er/Bi). Also, with the increase in the concentration of erbium ions there is an expansion in a volume of unit cell, an increase in the orthorhombic distortion and orthorhombicity followed by the increase in tetragonal strain.

Table 1. Lattice parameters of $SrBi_{2-x}Nb_2Er_xO_9$

$SrBi_{2-x}Nb_2Er_xO_9$	a(Å)	b(Å)	c(Å)	Volume(Å^3)	Orthorhombic Distortion, b/a	Orthorhombicity, 2(a-b)/(a+b)	Tetragonal strain, c/a
***x* = 0.00**	5.4933	5.5136	25.035	758.2565	1.003695	0.00369	4.55737
***x* = 0.01**	5.4938	5.5141	25.039	758.5155	1.003695	0.00369	4.557683
***x* = 0.02**	5.4943	5.5146	25.043	758.7745	1.003695	0.00369	4.557996
***x* = 0.03**	5.4946	5.5152	25.047	759.0197	1.003749	0.00374	4.558476
***x* = 0.04**	5.4949	5.5157	25.051	759.2512	1.003785	0.00378	4.558955
***x* = 0.05**	5.4951	5.5162	25.055	759.4689	1.003840	0.00383	4.559517

4.2 SEM and EDS

Morphology and compositional analysis of synthesized pure SBN have been investigated along with the Energy-dispersive spectrum (EDS). Fig.5 shows SEM image of pure SBN ceramic pellet with their EDS graph. The micrograph shows the formation of grains that are randomly oriented with a presence of porosity in the microstructure as the solid-state method leads to more pores and non-uniform grain size, and the dense sample was achieved underprepared conditions. Porosity leads to conductivity and has some application such as thermal stability, high permeability, and high resistance to chemical attack. Moreover, due to high-density growth, agglomerations in the nanoparticles were also seen. The energy dispersive spectroscopy (EDS) was used for elemental analysis and from the analysis the information obtained was that no other impurity elements were detected confirms the absence of secondary phases in the required sintered sample and those detected elements: O, Sr, Bi, and Nb were present in the desired composition in the sample, described in table 2. Fig. 6 shows the EDS graph of pure SBN.

Table 2. Composition of elements present in pure SBN, sintered at 1000℃.

Element	Weight %	Weight % (σ)	Atomic %
Oxygen	21.212	0.983	69.781
Strontium	9.541	0.544	5.731
Niobium	22.402	0.868	12.691
Bismuth	46.844	1.154	11.797

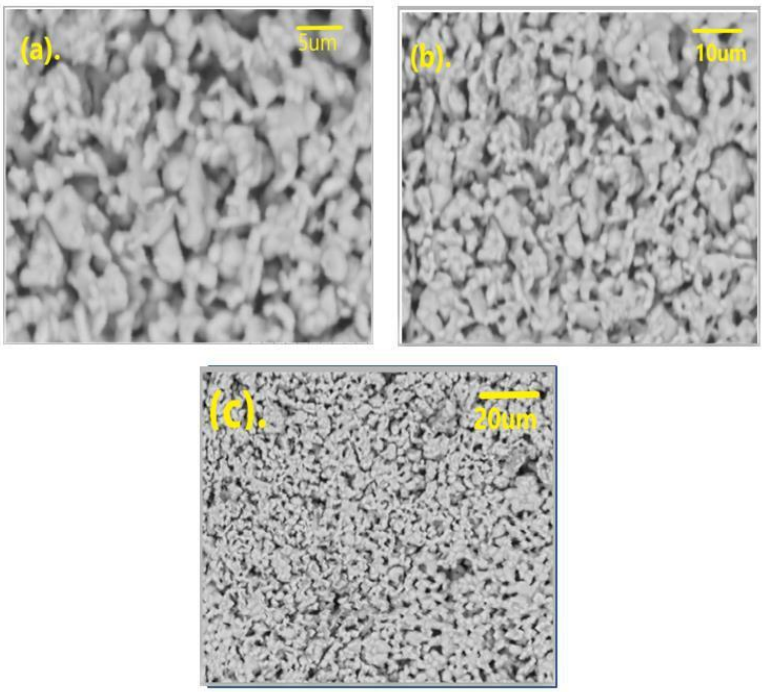

Fig.5 SEM image of pure SBN.

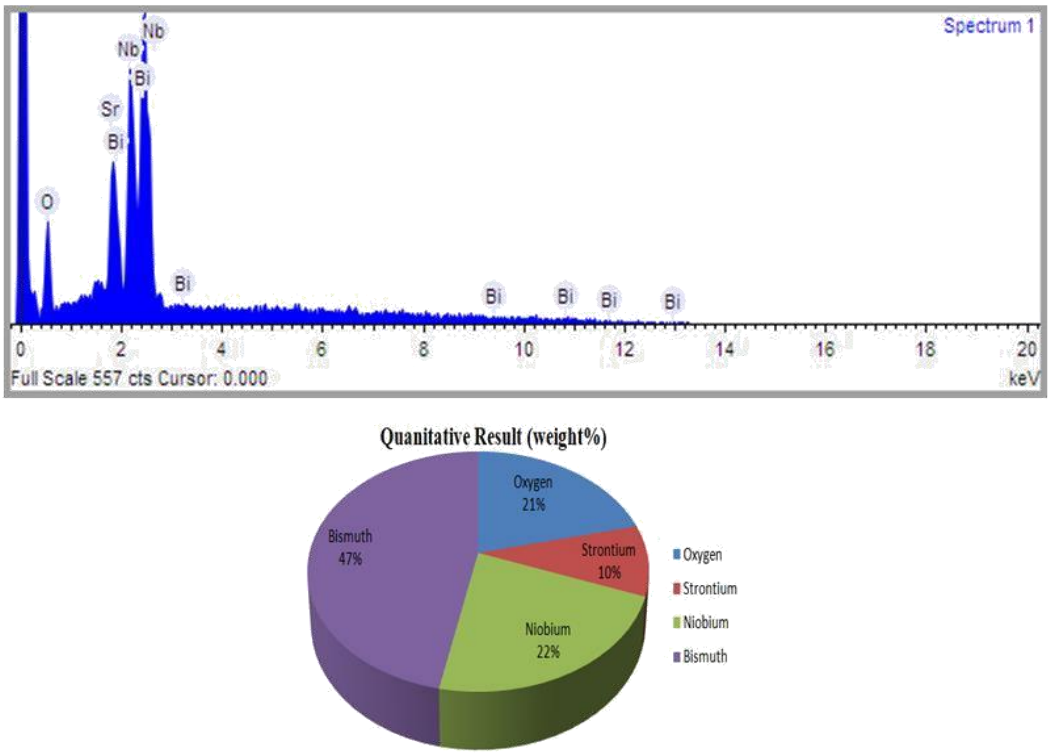

Fig.6. EDS graph of pure SBN

The micrographs indicated insignificant changes in grain size with varying increasing Er content. The compositional analysis of pure $SrBi_2Nb_2O_9$ and Er^{3+} doped $SrBi_{2-x}Nb_2Er_xO_9$ pellets was done by EDS (Energy Dispersive Spectrum) and the data of the elements were given in the Table 3.

Table 3: EDS compositional analysis

Nominal Composition	Sr (at%)	Bi (at%)	Nb (at%)	Er (at%)	Er/Bi
Stoichiometric $SrBi_2Nb_2O_9$	5.731	11.797	12.691	-	-
Present Work $SrBi_{2-x}Nb_2Er_xO_9$					
x					
0.00	3.53	11.151	6.363	-	-
0.01	2.652	8.328	4.775	0.034	0.004
0.02	2.653	8.319	4.777	0.068	0.008
0.03	2.654	8.253	4.779	0.103	0.012
0.04	2.656	8.215	4.782	0.137	0.016
0.05	2.657	8.177	4.784	0.172	0.021

4.3 Raman Scattering Study

Raman Spectroscopy, chemical analysis technique based on the interaction of light with the chemical bonds present within a material. Raman spectroscopy is utilized for investigating the basic lattice symmetry, crystal structure, and molecular interactions of ferroelectric compounds. Fig.7. shows the Raman Spectra of sintered SrBi2Nb2O9 (pure SBN) ceramic pellet, at room temperature within the spectral range 100 cm^{-1} to 1000 cm^{-1}. Some intense peaks can be seen at 205.4 cm^{-1}, 578.59 cm^{-1} and 833.90 cm^{-1} with relatively large Raman intensity, apart from that some weak peaks are also observed at 176.06 cm^{-1}, 272.16 cm^{-1}, 448.87 cm^{-1} and 709.57 cm^{-1}. The 176.06cm^{-1} mode corresponds to Nb z-axis vibrations, modes at 205.4 cm^{-1} attributed to the Bi^{3+} vibrations or related to the vibrations of A-site ions. The mode at 272.16 cm^{-1} is leading by a force constant due to Bi-O2 and Nb-Bi-O2 bonds. The mode at 449.87 cm^{-1} moved to low frequency for scanty Sr. The mode at 709.57 cm^{-1} assigns to asymmetric distortion of BO3 triangular group and BO4 tetrahedron. Also, mode at 578.59 cm^{-1} corresponds to a rigid sub-lattice mode where the displacement of positive and negative ion displacement is equal and opposite. The mode located at 833.90 cm^{-1} reflects symmetric stretching of the octahedral NbO6 and the presence of NbO6 clearly indicates the predominance of the orthorhombic phase. So, at 176.06 cm^{-1} 205.4 cm^{-1}, 578.59 cm^{-1}, and 833.90 cm^{-1} modes related to the orthorhombic phase which is in agreement with the XRD pattern.

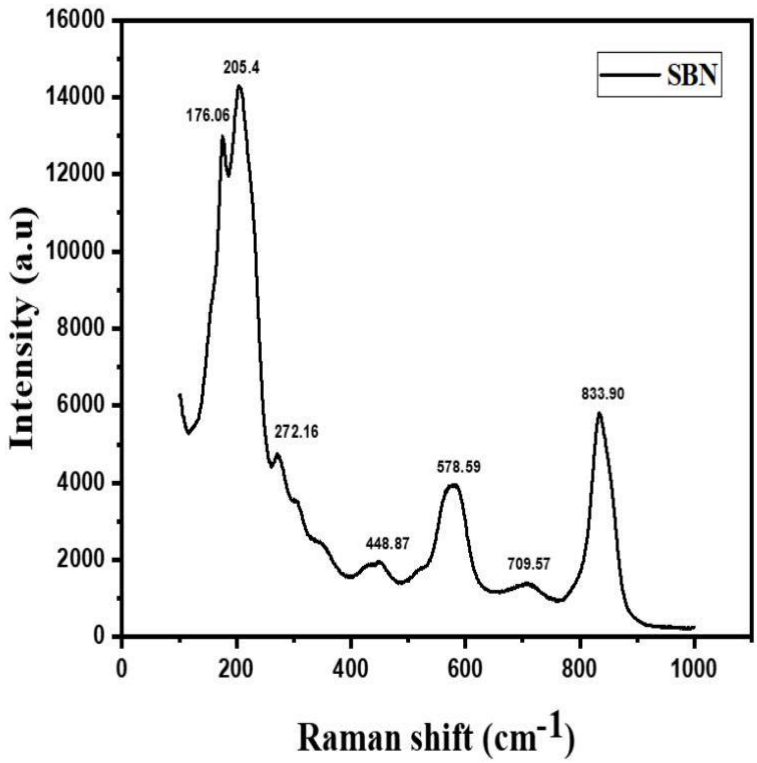

Fig.7. Raman Spectra of SBN ceramics at spectral range 100cm^{-1} to 1000cm^{-1}.

4.4 Photoluminescence spectra

The photoluminescence (PL) properties of Er^{3+} doped SrBi2-*x*Nb2Er*x*O9 (*x* = 0.00, 0.01, 0.02, 0.03, 0.04 and 0.05) ceramics for different concentrations were examined under the excitation wavelength, λex = 480 nm at room temperature and acquired photoluminescence emission spectrum is shown in Fig.8. From the observations, all the Er doped SrBi2-xNb2ErxO9 ceramics display strong green emission ranging from 529.2 nm to 549.8 nm, (centred at 529.2 nm, 540.96 nm, 542.95 nm, and 549.8 nm) refers ^{2}H11/2→^{4}I15/2, and ^{4}S3/2→^{4}I15/2 transitions, respectively and light greenish emission was observed at 579.4 nm. Furthermore, the splitting of PL spectra ranging from 540.96 nm to 549.8 nm into several components is due to Stark effect (or Stark splitting). The highest peak of PL emission spectra monitored at a wavelength of 549.8 nm i.e., the strong green emission refers to the excitation of Er^{3+} ions from ground level ^{4}I15/2 to higher energy level ^{4}S3/2 rather than the host material. With an increase in the doping content of Er^{3+} firstly, the PL intensity increases up to *x* = 0.03 and then decreases because by means of concentration quenching while the position of emission peaks for all remains the same. As indicated in PL spectra, the maximum emission intensity occurs at a concentration, *x* = 0.03. So, Er^{3+} doped SrBi2-*x*Nb2Er*x*O9 (x=0.00, 0.01, 0.02, 0.03, 0.04 and 0.05) ceramics can be considered as appropriate visible light excited green phosphors where Er^{3+} doped SrBi2-*x*Nb2Er*x*O9 with concentration, x=0.03 ceramics outshines others.

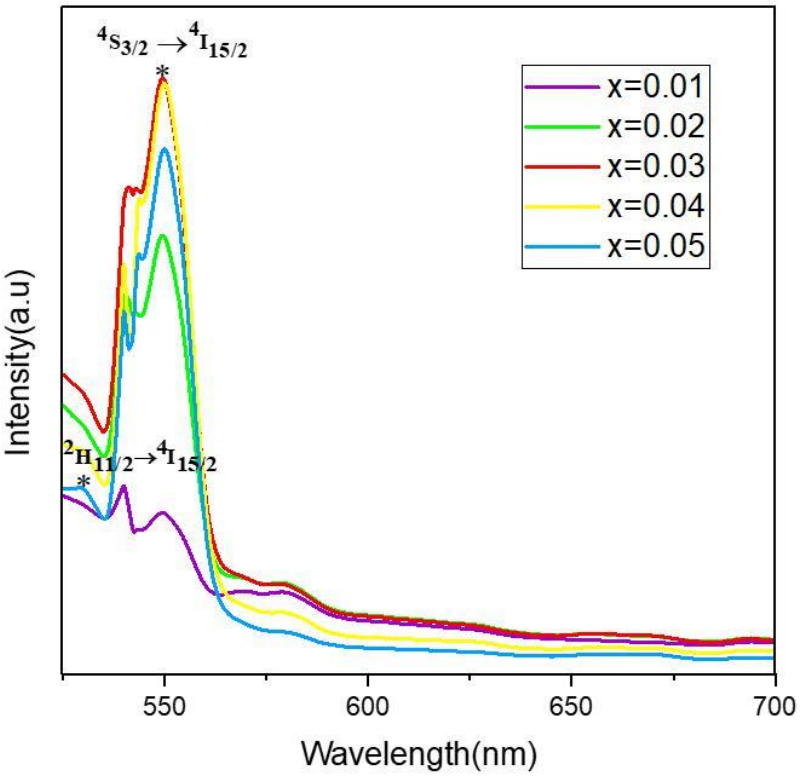

Fig.8. PL spectra of Er^{3+} doped SrBi2-xNb2ErxO9 at different concentrations under 480nm excitation wavelength

Chapter 5:

Conclusions

Pure SBN ceramic prepared by the conventional solid-state method was investigated to study the evolution of phases during the single-phase formation of pure SBN when the sample undergoes heat treatment at different calcination temperatures: 800ºC, 850°C, and 950ºC. XRD spectra reveal with an increase in the calcination temperature, the intensity of intermediate phases decreases and at 950°C no impurity phases were detected and show the formation of peaks of a single phase of SrBi2Nb2O9 with orthorhombic geometry, followed by the calcination of Er^{3+} doped SBN at different concentrations. Then all pure and Er^{3+} doped SBN samples sintered at 1000ºC. The study of XRD patterns of pure SBN and Er^{3+} doped SBN indicates that the pure SBN is orthorhombic in nature with no secondary phases and with further increase in the doping concentration of Er^{3+} ion in SBN results in the shifting of strongest peak (115) towards lower angles and there is an increase in orthorhombic distortion and orthorhombicity with the increase in Er content. The Surface micrograph shows the formation of grains that are randomly oriented with a presence of porosity in the microstructure and the elemental analysis by EDS reveals that only elements O, Sr, Bi, and Nb were detected in the desired composition. The Raman study shows the SBN orthorhombic phase and the modes located at 176.06cm^{-1} 205.4cm^{-1}, 578.59cm $^{-1}$, and 833.90 cm^{-1} related to the orthorhombic phase of pure SBN. The synthesis of Er^{3+} doped SrBi2Nb2O9 ceramics, their structural analysis and PL properties were investigated and studied. The PL properties implies, at a 480 nm excitation wavelength, strong green emission bands observed at 549.8 nm and strongest emission intensity was achieved at a concentration of Er^{3+} when x = 0.03.

REFERENCES

[1] G. H. Haertling, "<1999 Ferroelectrics, history and technology, Haertling-1999-Journal_of_the_American_Ceramic_Society.pdf>," *J. Am. Ceram. Soc.*, vol. 82, pp. 797–818, 1999.

[2] J. F. Scott, "Applications of modern ferroelectrics," *Science (80-.).*, vol. 315, no. 5814, pp. 954–959, 2007, doi: 10.1126/science.1129564.

[3] M. A. Peña and J. L. G. Fierro, "Chemical structures and performance of perovskite oxides," *Chem. Rev.*, vol. 101, no. 7, pp. 1981–2017, 2001, doi: 10.1021/cr980129f.

[4] Z. Peng *et al.*, "Crystal structure, dielectric and piezoelectric properties of Ta/W codoped Bi3TiNbO9 Aurivillius phase ceramics," *Curr. Appl. Phys.*, vol. 14, no. 12, pp. 1861–1866, 2014, doi: 10.1016/j.cap.2014.10.011.

[5] S. Zhang and F. Yu, "Piezoelectric materials for high temperature sensors," *J. Am. Ceram. Soc.*, vol. 94, no. 10, pp. 3153–3170, 2011, doi: 10.1111/j.1551-2916.2011.04792x.

[6] P. H. Abelson, "Materials research," *Science (80-.).*, vol. 235, no. 4784, p. 9, 1987, doi: 10.1126/science.235.4784.9.

[7] P. Yang, D. L. Carroll, J. Ballato, and R. W. Schwartz, "Growth and optical properties of SrBi2Nb2O9 ferroelectric thin films using pulsed laser deposition," *J. Appl. Phys.*, vol. 93, no. 11, pp. 9226–9230, 2003, doi: 10.1063/1.1571219.

[8] A. Ando, T. Sawada, H. Ogawa, M. Kimura, and Y. Sakabe, "Fine-tolerance resonator applications of bismuth-layer-structured ferroelectric ceramics," *Japanese J. Appl. Physics, Part 1 Regul. Pap. Short Notes Rev. Pap.*, vol. 41, no. 11 B, pp. 7057–7061, 2002, doi: 10.1143/JJAP.41.7057.

[9] A. Banwal and R. Bokolia, "Phase evolution and microstructure of BaBi2Nb2O9 ferroelectric ceramics," *Mater. Today Proc.*, vol. 3, no. xxxx, pp. 2–5, 2020, doi: 10.1016/j.matpr.2020.09.380.

[10] M. Verma, A. Tanwar, and K. Sreenivas, "Phase evolution of strontium bismuth niobate ceramics by conventional solid-state reaction method," *J. Therm. Anal. Calorim.*, vol. 135, no. 4, pp. 2077–2087, 2019, doi: 10.1007/s10973-018-7287-7.

[11] D. P. Volanti *et al.*, "The role of the Eu3+ ions in structure and photoluminescence properties of SrBi2Nb2O9 powders," *Opt. Mater. (Amst).*, vol. 31, no. 6, pp. 995– 999, 2009, doi: 10.1016/j.optmat.2008.11.006.

[12] M. K. Adak, A. Mukherjee, A. Chowdhury, J. Khatun, U. K. Ghorai, and D. Dhak, "Electrical and energy storage properties of nickel substituted barium bismuth niobate nano-ceramics prepared by chemical route," *J. Mater. Sci. Mater. Electron.*, vol. 29, no. 18, pp. 15847–15858, 2018, doi: 10.1007/s10854-018-9671-2.

[13] D. P. Volanti *et al.*, "Photoluminescent behavior of Sr Bi2 Nb2 O9 powders explained by means of B- Bi2 O3 phase," *Appl. Phys. Lett.*, vol. 90, no. 26, pp. 1–4, 2007, doi: 10.1063/1.2753114.

[14] G. Z. Liu, C. Wang, H. S. Gu, and H. Bin Lu, “Raman scattering study of La-doped SrBi2Nb2O 9 ceramics,” *J. Phys. D. Appl. Phys.*, vol. 40, no. 24, pp. 7817–7820, 2007, doi: 10.1088/0022-3727/40/24/034.

[15] Y. Zhao, X. Wang, Y. Zhang, Y. Li, and X. Yao, “Optical temperature sensing of up-conversion luminescent materials: Fundamentals and progress,” *J. Alloys Compd.*, vol. 817, p. 152691, 2020, doi: 10.1016/j.jallcom.2019.152691.

[16] D. P. Volanti *et al.*, “The role of the Eu3+ ions in structure and photoluminescence properties of SrBi2Nb2O9 powders,” *Opt. Mater. (Amst).*, vol. 31, no. 6, pp. 995– 999, 2009, doi: 10.1016/j.optmat.2008.11.006.

[17] T. Wei *et al.*, “Enhanced up-conversion photoluminescence and dielectric properties of Er- and Zr-codoped strontium bismuth niobate ceramics,” *Ceram. Int.*, vol. 41, no. 9, pp. 12364–12370, 2015, doi: 10.1016/j.ceramint.2015.06.067.

[18] D. Peng, H. Sun, X. Wang, J. Zhang, M. Tang, and X. Yao, “Red emission in Pr doped CaBi4Ti4O15 ferroelectric ceramics,” *Mater. Sci. Eng. B Solid-State Mater. Adv. Technol.*, vol. 176, no. 18, pp. 1513–1516, 2011, doi: 10.1016/j.mseb.2011.09.009.

[19] V. Senthil, T. Badapanda, A. Chandra Bose, and S. Panigrahi, “Enhancement of dielectric and ferroelectric properties of dysprosium substituted SrBi2Ta2O9 ceramics,” *J. Mater. Sci. Mater. Electron.*, vol. 27, no. 2, pp. 1602–1608, 2016, doi: 10.1007/s10854-015-3930-2.

[20] S. Jain, P. Ganguly, S. Devi, and A. K. Jha, “Structural, dielectric and ferroelectric studies of molybdenum substituted Sr2Bi2Nb2O9 ferroelectric ceramics,” *Ferroelectrics*, vol. 381, no. 1 PART 2, pp. 152–159, 2009, doi: 10.1080/00150190902870051.

[21] O. Jalled *et al.*, “Synthesis and dielectric properties of nanocrystalline strontium bismuth niobate,” *J. Nanosci. Nanotechnol.*, vol. 17, no. 1, pp. 594–600, 2017, doi: 10.1166/jnn.2017.12459.

[22] L. Yu, J. Hao, Z. Xu, W. Li, R. Chu, and G. Li, “Strong photoluminescence and good electrical properties in Eu-modified SrBi2Nb2O9 multifunctional ceramics,” *Ceram. Int.*, vol. 42, no. 13, pp. 14849–14854, 2016, doi: 10.1016/j.ceramint.2016.06.119.

[23] T. Wei, C. Z. Zhao, Q. J. Zhou, Z. P. Li, Y. Q. Wang, and L. S. Zhang, “Bright green upconversion emission and enhanced ferroelectric polarization in Sr1-1.5xErxBi2Nb 2O9,” *Opt. Mater. (Amst).*, vol. 36, no. 7, pp. 1209–1212, 2014, doi: 10.1016/j.optmat.2014.03.001.

[24] P. Henderson, “Rare earth element geochemistry, Developments in geochemistry,” vol. 2, p. 510, 1984, [Online]. Available: http://ezproxy.lib.utexas.edu/login?url=http://search.ebscohost.com/login.aspx?direct=true&db=geh&AN=1984-023694&site=ehost-live.

[25] A. Tomar, M. Singh, S. Singh, L. Sharma, S. Arya, and S. Kasana, “Ultraviolet Quantum Cutting through down Conversion Luminescence Behaviour of Er3+ Substituted Sr0.7Bi2.2Nb2O9 (BLFS) Ceramics,” *Integr. Ferroelectr.*, vol. 204, no. 1, pp. 33–37, 2020, doi: 10.1080/10584587.2019.1674983.

[26] T. Honma, T. Komatsu, D. Zhao, and H. Jain, “Writing of rare-earth ion doped lithium niobate line patterns in glass by laser scanning,” *IOP Conf. Ser. Mater. Sci. Eng.*, vol. 1, p. 012006, 2009, doi: 10.1088/1757-8981/1/1/012006.

[27] L. Mukhopadhyay, V. K. Rai, R. Bokolia, and K. Sreenivas, “980 nm excited Er3+/Yb3+/Li+/Ba2+: NaZnPO4 upconverting phosphors in optical thermometry,” *J. Lumin.*, vol. 187, no. October, pp. 368–377, 2017, doi: 10.1016/j.jlumin.2017.03.035.

[28] R. Bokolia, O. P. Thakur, V. K. Rai, S. K. Sharma, and K. Sreenivas, “Dielectric, ferroelectric and photoluminescence properties of Er3+ doped Bi4Ti3O12 ferroelectric ceramics,” *Ceram. Int.*, vol. 41, no. 4, pp. 6055–6066, 2015, doi: 10.1016/j.ceramint.2015.01.062.

RESEARCH PAPERS

1.

Materials Today: Proceedings xxx (xxxx) 1–5

Contents lists available at ScienceDirect

Materials Today: Proceedings

journal homepage: http://ees.elsevier.com

Structural properties of Strontium Bismuth Niobate ($SrBi_2Nb_2O_9$) ferroelectric ceramics

Pooja Mojumdar, Ritushree Shaily, Renuka Bokolia*

Department of Applied Physics, Delhi Technological University, New Delhi, India

ARTICLE INFO

Article history:
Received 31 March 2021
Received in revised form 22 May 2021
Accepted 24 May 2021
Available online xxx

Keywords
SBN
Phase evolution
XRD
Ferroelectric
Raman
Ceramics

ABSTRACT

The pure $SrBi_2Nb_2O_9$ (SBN) ceramic was synthesized by the conventional solid-state reaction method. The sample was then undergoing heat treatment at different calcination temperatures: 800 °C, 850 °C, and 950 °C, and the evolution of phases were studied at these different calcination temperatures, followed by sintering at 1000 °C of temperature to form single-phase SBN. Few secondary phases have been identified along with the desired SBN phase but begin to decrease with the increase in the calcination temperature. The most appropriate calcination and sintering temperature have been successfully investigated with no impurity phase. The structural morphology of the sample sintered at 1000 °C studied under SEM reveals the formation of the highly dense plate-like grains and EDS provides information about the elemental composition. The Raman analysis revealed the formation of the orthorhombic phase of pure SBN.

1. Introduction

Ferroelectric ceramics were the backbone of billion-dollar industries from the high-dielectric capacitor to positive temperature coefficient devices and electro-optic valves because they have great features such as high dielectric permittivity, outstanding piezoelectric response, and swappable macroscopic polarization [1,2]. The goal to achieve better electronic device technology and higher efficient energy production devices was the main focus for rapid development in ferroelectric oxide ceramics. Oxides with Perovskite structure have general formula ABO_3 where A is a large positive ion with 12-fold coordinate and B is a small negative ion with 6-fold coordinated with oxygen anions have been broadly studied in the search of new material for device application [3]. After a detailed study of ferroelectric, we found BSLF (Bismuth layered ferroelectric) has gained much momentum for its properties such as high curie temperature coefficient, low ageing rate, and electro-optic behaviour. BSLF has great potential in electronic devices. BSLF are from the Aurivillius family having formula $(Bi_2O_2)^{2+}(A_{n-1}B_nO_{3n+1})^{2-}$ where $(Bi_2O_2)^{2+}$ is bismuth layer and $(A_{n-1}B_nO_{3n+1})^{2-}$ is pseudo perovskite layer. The A site is supposed to be occupied by cation Na^+, K^+, Sr^{2+}, Ca^{2+}, Ba^{2+}, Ba^{3+} and B site is occupied by W^{6+}, Nb^{5+}, Ti^4, etc. [4]. Bismuth layer ferroelectric having n = 2 i.e., $CaBi_2Nb_2O_9$ (CBN), $BaBi_2Nb_2O_9$ (BBN), $SrBi_2Nb_2O_9$(SBN) have many properties like the low operating voltage, excellent switching speed, small leakage current density. Two-layer Aurivillius compound (n = 2) has a high curie temperature ≥ 900 °C so they have the best application in spacecraft, aerospace, and nuclear plants [5]. The two-layer Aurivillius family has one of the most important ceramic compounds Strontium Bismuth Niobate ($SrBi_2Nb_2O_9$). $SrBi_2Nb_2O_9$ is a BSLF material that has special importance due to its anti- fatigue property, spontaneous polarization, and low-temperature coefficient of resonance frequency [6]. $SrBi_2Nb_2O_9$ has great application in non-volatile random-access memory and in fine frequency tolerance resonators [7–8]. SBN is a lead-free relaxor ceramic. All these properties have inspired us to synthesize Strontium Bismuth Niobate. In the present, we study variations in phase evolution at different calcination temperatures during the preparation of $SrBi_2Nb_2O_9$ ceramic to get a single-phase SBN with no impurity phase.

2. Experimental details

2.1. Synthesis

Pure Strontium Bismuth Niobate ($SrBi_2Nb_2O_9$) sample was synthesized by the conventional solid-state method [9]. Firstly, high purity raw materials: $SrCO_3$ (~99.9%), Nb_2O_5 (~99.9%), and Bi_2O_3 (~99.7%) were stoichiometrically weighed and then mixed. The mixture of powders was grinded for 6 h followed by calcination. The grinded powder was calcinated at three different calcination temperatures: 800 °C, 850 °C, and 950 °C with a hold of 3 h. The calcined powder was rigorously mixed with 5% wt. polyvinyl alcohol, a binder, and then the resulting powder was converted into disc-shaped pellets of thickness 1 mm with a diameter of 13 mm manually by the hydraulic press at a pressure of 50 MPa with 1 min resting time. After that, the pellets were finally sintered at 1000 °C for 8 h with intermediate heat treatment at

* Corresponding author.
E-mail address: renukabokolia@dtu.ac.in (R. Bokolia)

https://doi.org/10.1016/j.matpr.2021.05.522
2214-7853/© 2021.

500 °C for 1 h so that there will be no traces of binder left in the sample. The equation for synthesis:

$$SrCO_3 + Bi_2O_3 + Nb_2O_5 \rightarrow SrBi_2Nb_2O_9 + CO_2 \uparrow$$

2.2. Characterization techniques

The crystallographic structural analysis of pure SBN was studied under X-Ray diffraction (XRD, Bruker D8 Advance X-ray diffractometer) using Cu-Kα radiation (λ = 0.154 nm). The XRD spectrum was observed within the range, 20°≤2θ≤70°. The peak of ceramics was matched with JCPDF file number 01–089-8154 to confirm the pure phase of SBN. The crystalline size has been calculated by Scherrer's equation:

$$D = \frac{0.89\lambda}{\beta cos\theta}$$

where, D is the average crystalline size, λ is Cu-Kα$_1$(λ = 0.154 nm) wavelength, β is the full width at half maximum (FWHM) of the diffraction peak, and θ is the angle of diffraction.

The structural morphology and grain formation have been investigated on unpolished sintered ceramic pellets by using the JEOL 661 Scanning electron microscopy (SEM) equipped with Amkette energy dispersive spectrometer (EDS). At room temperature, the Raman spectra were recorded by using the Horiba LabRam HR evolution spectrometer at wavelength 514 nm at 40 mW.

3. Result and discussion

3.1. X-Ray diffraction analysis

Fig. 1(a, b, c) depicts the evolution of phase that develops during the calcinations heat treatment at 800 °C, 850 °C, and 950 °C of $SrBi_2Nb_2O_9$(SBN) powder to form a single-phase of SBN. The calcination temperature uprises to 1000 °C to ensure that single-phase SBN ($SrBi_2Nb_2O_9$) is formed. Highly pure raw materials $SrCO_3$, Nb_2O_5, and Bi_2O_3 were mixed stoichiometrically, as the reaction between them proceeds to lead to the formation of various intermediate phases accompanying the initial crystallization of $SrBi_2Nb_2O_9$ phase. During the reaction between Bi_2O_3 and Nb_2O_5 numerous phases e.g., $Bi_6Nb_{18}O_{57}$, $BiNbO_4$ and $Bi_5Nb_3O_{15}$ are formed [10]. At 800 °C calcined temperature, the XRD pattern shows the presence of Bi_2O_3, $SrBi_2O_4$ (due to the reaction between Bi_2O_3 and $SrCO_3$), single-phase $Bi_5Nb_3O_{15}$, and some intermediate phase of $BiNbO_4$, existed side by side with desired single-phase $SrBi_2Nb_2O_9$ phase and the same intermediate phases were also detected at 850 °C. At 850 °C, the XRD pattern shows the mix phase of $SrBi_2Nb_2O_9$ and Bi_2O_3 at 28.82° & 29.06° respectively. From the literature survey, we found that peaks corresponding to Bi_2O_3 phase seen at 2θ (31.66°, 47.08°, and 58.06°) because Bi_2O_3 remains unreacted but when it is treated to a higher range of temperature, the phase of Bi_2O_3 disappears. Also, it is interesting to see that intermediate phases i.e., $SrBi_2O_4$, $Bi_5Nb_3O_{15}$, and $BiNbO_4$ start decreasing with the increase in the calcination temperature. When the calcination temperature rises to 950 °C no secondary phases are observed for the sample indicating that the reaction mechanism for the phase evolution of pure SBN is com-

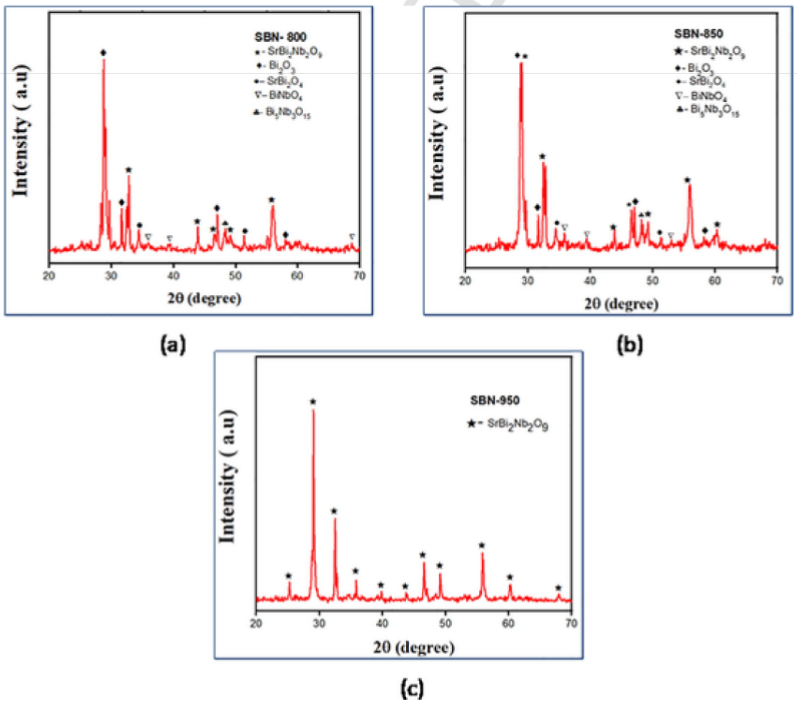

Fig. 1. XRD pattern of $SrBi_2Nb_2O_9$ at different temperature (a) at 800 °C (b) 850 °C (c) 950 °C.

pleted followed by sintering at 1000 °C. The peak of ceramics is matched with JCPDF file number 01-089-8154 confirms the pure SBN of single-phase and no secondary phases were detected. Thus, the reaction mechanism for obtaining the desire phase of $SrBi_2Nb_2O_9$, should be calcinated at 950 °C and sintered at 1000 °C. (Fig. 2). The lattice parameters for pure SBN a = 5.4933 Å, b = 5.5136 Å, and c = 25.035 Å related to the orthorhombic phase, associated with the space group $A2_1am$. The lattice parameter was calculated with the help of PowderX software. Also, the highest diffraction peak associated with the (1 1 5) plane of $SrBi_2Nb_2O_9$ was detected. The average crystallite size of SBN was calculated by Scherrer's equation which is found to be 31.50 nm. As the intensity and sharpness of the peak increases with an increase in temperature attributed to increase in crystallinity.

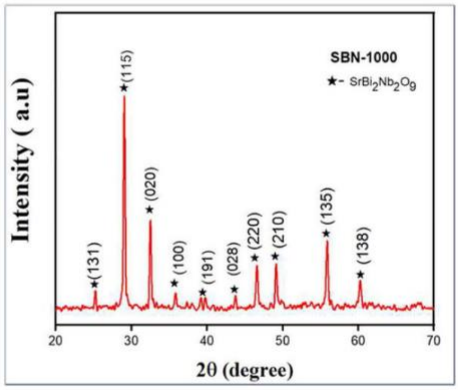

Fig. 2. XRD pattern of $SrBi_2Nb_2O_9$ ceramic pellet sintered at temperature 1000 °C.

3.2. SEM and EDS analysis

Morphology and compositional analysis of synthesized pure SBN have been investigated along with the Energy-dispersive spectrum (EDS). Fig. 3 shows SEM image of pure SBN ceramic pellet with their EDS graph. The micrograph shows the formation of grains that are randomly oriented with a presence of porosity in the microstructure as the solid-state method leads to more pores and non-uniform grain size, and the dense sample was achieved underprepared conditions. Porosity leads to conductivity and has some application such as thermal stability, high permeability, and high resistance to chemical attack. Moreover, due to high-density growth, agglomerations in the nanoparticles were also seen [11,12]. The energy dispersive spectroscopy (EDS) was used for elemental analysis and from the analysis the information obtained was that no other impurity elements were detected confirms the absence of secondary phases in the required sintered sample and those

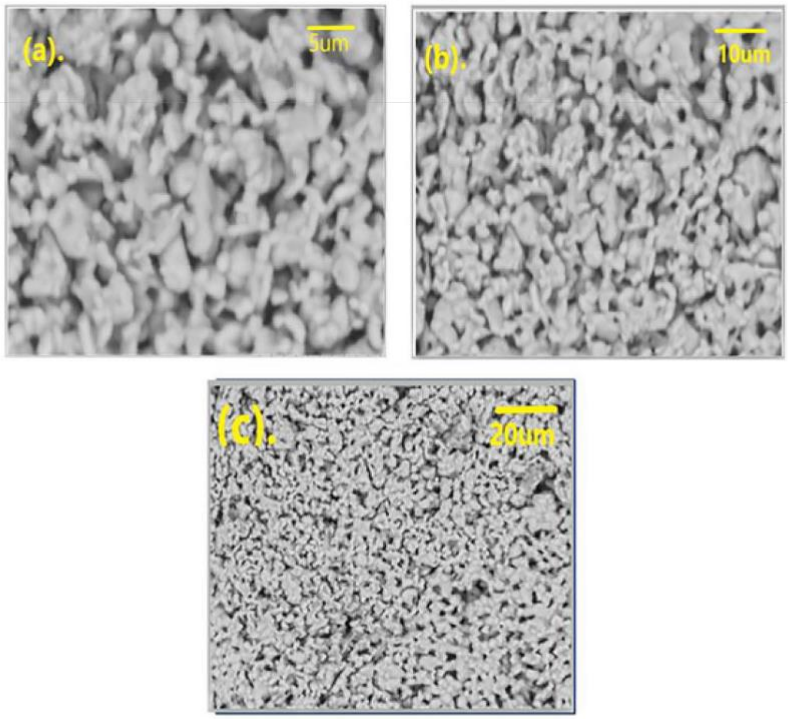

Fig. 3. SEM image of pure SBN.

Table 1
Composition of elements present in pure SBN, sintered at 1000 °C.

Element	Weight %	Weight % (σ)	Atomic %
Oxygen	21.212	0.983	69.781
Strontium	9.541	0.544	5.731
Niobium	22.402	0.868	12.691
Bismuth	46.844	1.154	11.797

detected elements: O, Sr, Bi, and Nb were present in the desired composition in the sample, described in Table 1. (See Fig. 4.)

3.3. Raman scattering study

Raman Spectroscopy, chemical analysis technique based on the interaction of light with the chemical bonds present within a material. Raman spectroscopy is utilized for investigating the basic lattice symmetry, crystal structure, and molecular interactions of ferroelectric compounds. Fig. 5 shows the Raman Spectra of sintered SrBi2Nb2O9 (pure SBN) ceramic pellet, at room temperature within the spectral range 100 cm^{-1} to 1000 cm^{-1}. Some intense peaks can be seen at 205.4 cm^{-1}, 578.59 cm^{-1} and 833.90 cm^{-1} with relatively large Raman intensity, apart from that some weak peaks are also observed at 176.06 cm^{-1}, 272.16 cm^{-1}, 448.87 cm^{-1} and 709.57 cm^{-1}. The 176.06 cm^{-1} mode corresponds to Nb z-axis vibrations, modes at 205.4 cm^{-1} attributed to the Bi^{3+} vibrations or related to the vibrations of A-site ions. The mode at 272.16 cm^{-1} is leading by a force constant due to Bi-O_2 and Nb-Bi-O_2 bonds. The mode at 449.87 cm^{-1} moved to low frequency for scanty Sr. The mode at 709.57 cm^{-1} assigns to asymmetric deformation of BO_3 triangular group and distortion of BO_4 tetrahedron Also, mode at 578.59 cm^{-1} corresponds to a rigid sub-lattice mode where the displacement of positive and negative ion displacement is equal and opposite. The mode located at 833.90 cm^{-1} reflects symmetric stretching of the octahedral NbO_6 and the presence of NbO_6 clearly indicates the predominance of the orthorhombic phase. So, at 176.06 cm^{-1} 205.4 cm^{-1}, 578.59 cm^{-1}, and 833.90 cm^{-1} modes related to the orthorhombic phase which is in agreement with the XRD pattern [13–16].

4. Conclusion

Pure SBN ceramic prepared by the conventional solid-state method was investigated to study the effect of different calcination temperatures: 800 °C, 850°C, and 950 °C, on the evolution of phases during the single-phase formation of pure SBN. XRD spectra reveal with an increase in the calcination temperature, the intensity of intermediate phases decreases and at 950°C no impurity phases were detected and show the formation of peaks of a single phase of $SrBi_2Nb_2O_9$ with orthorhombic geometry, followed by the sintering of the sample at 1000 °C. The Surface micrograph shows the formation of grains that are randomly oriented with a presence of porosity in the microstructure and the elemental analysis by EDS reveals that only elements O, Sr, Bi, and Nb were detected in the desired composition. The Raman study shows the SBN orthorhombic phase and the modes located at 176.06 cm^{-1} 205.4 cm^{-1}, 578.59 cm^{-1}, and 833.90 cm^{-1} related to the orthorhombic phase of pure SBN.

CRediT authorship contribution statement

Pooja Mojumdar: Conceptualization, Methodology, Investigation, Data curation, Writing - original draft. **Ritushree Shaily:** Conceptualization, Methodology, Investigation, Data curation, Writing - original draft. **Renuka Bokolia:** Conceptualization, Methodology, Writing - original draft, Writing - review & editing, Supervision.

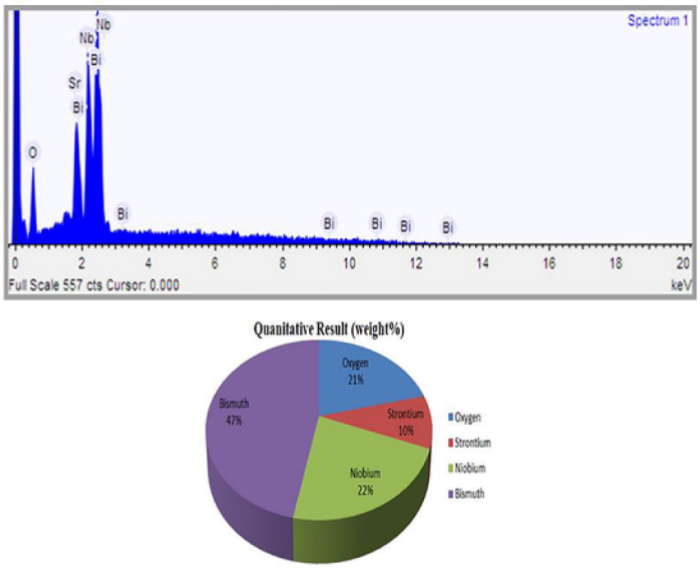

Fig. 4. EDS graph of pure SBN.

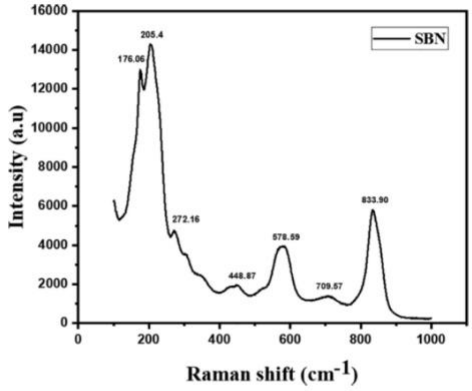

Fig. 5. Raman Spectra of SBN ceramics at spectral range 100 cm^{-1} to 1000 cm^{-1}.

Declaration of Competing Interest

The authors declare that they have no known competing financial interests or personal relationships that could have appeared to influence the work reported in this paper.

Acknowledgments

I would like to thank Research Project Grant (F.NO. DTU/IRD/619/2019/2112) Delhi Technological University for providing the research facilities and acknowledged technical staff, AIC, Department of Applied Physics for aiding with the characterization of the samples.

References

[1] G.H. Haertling, <1999 Ferroelectrics, history and technology, Haertling-1999-Journal_of_the_American_Ceramic_Society.pdf>, J. Am. Ceram. Soc. 82 (1999) 797–818.
[2] J.F. Scott, Applications of modern ferroelectrics, Science (80-.) 315 (5814) (2007) 954–959, doi:10.1126/science.1129564.
[3] M.A. Peña, J.L.G. Fierro, Chemical structures and performance of perovskite oxides, Chem. Rev. 101 (7) (2001) 1981–2017, doi:10.1021/cr980129f.
[4] Z. Peng, D. Yan, Q. Chen, D. Xin, D. Liu, D. Xiao, J. Zhu, Crystal structure, dielectric and piezoelectric properties of Ta/W codoped Bi3TiNbO9 Aurivillius phase ceramics, Curr. Appl. Phys. 14 (12) (2014) 1861–1866, doi:10.1016/j.cap.2014.10.011.
[5] S. Zhang, F. Yu, Piezoelectric materials for high temperature sensors, J. Am. Ceram. Soc. 94 (10) (2011) 3153–3170, doi:10.1111/j.1551-2916.2011.04792x.
[6] P.H. ABELSON, Materials research, Science (80-.) 235 (4784) (1987) 9, doi:10.1126/science:235.4784.9.
[7] P. Yang, D.L. Carroll, J. Ballato, R.W. Schwartz, Growth and optical properties of SrBi2Nb2O9 ferroelectric thin films using pulsed laser deposition, J. Appl. Phys. 93 (11) (2003) 9226–9230, doi:10.1063/1.1571219.
[8] A. Ando, T. Sawada, H. Ogawa, M. Kimura, Y. Sakabe, Fine-tolerance resonator applications of bismuth-layer-structured ferroelectric ceramics, Japanese J. Appl. Physics, Part 1 Regul. Pap. Short Notes Rev. Pap. 41 (Part 1, No. 11B) (2002) 7057–7061, doi:10.1143/JJAP.41.7057.
[9] A. Banwal, R. Bokolia, Phase evolution and microstructure of BaBi2Nb2O9 ferroelectric ceramics, Mater. Today Proc. 3, xxxx (2020) 2–5, doi:10.1016/j.matpr.2020.09.380.
[10] M. Verma, A. Tanwar, K. Sreenivas, Phase evolution of strontium bismuth niobate ceramics by conventional solid-state reaction method, J. Therm. Anal. Calorim. 135 (4) (2019) 2077–2087, doi:10.1007/s10973-018-7287-7.
[11] D.P. Volanti, I.L.V. Rosa, E.C. Paris, C.A. Paskocimas, P.S. Pizani, J.A. Varela, E. Longo, The role of the Eu3+ ions in structure and photoluminescence properties of SrBi2Nb2O9 powders, Opt. Mater. (Amst) 31 (6) (2009) 995–999, doi:10.1016/j.optmat.2008.11.006.
[12] M.K. Adak, A. Mukherjee, A. Chowdhury, J. Khatun, U.K. Ghorai, D. Dhak, Electrical and energy storage properties of nickel substituted barium bismuth niobate nano-ceramics prepared by chemical route, J. Mater. Sci. Mater. Electron. 29 (18) (2018) 15847–15858, doi:10.1007/s10854-018-9671-2.
[13] D.P. Volanti, L.S. Cavalcante, E.C. Paris, A.Z. Simões, D. Keyson, V.M. Longo, A.T. de Figueiredo, E. Longo, J.A. Varela, F.S. De Vicente, A.C. Hernandes, Photoluminescent behavior of Sr Bi2 Nb2 O9 powders explained by means of B-Bi2 O3 phase, Appl. Phys. Lett. 90 (26) (2007) 261913, doi:10.1063/1.2753114.
[14] G.Z. Liu, C. Wang, H.S. Gu, H. Bin Lu, Raman scattering study of La-doped SrBi2Nb2O 9 ceramics, J. Phys. D Appl. Phys. 40 (24) (2007) 7817–7820, doi:10.1088/0022-3727/40/24/034.
[15] R. Singh, V. Luthra, R.S. Rawat, R.P. Tandon, Structural, dielectric and piezoelectric properties of SrBi2Nb2O9 and Sr0.8Bi2.2Nb2O9 ceramics, Ceram. Int. 41 (3) (2015) 4468–4478, doi:10.1016/j.ceramint.2014.11.139.
[16] H.C. Gupta, Archana, V. Luthra, Lattice vibrations of ABi2Nb2O9 crystals (A = Ca, Sr, Ba), Vib. Spectrosc. 56 (2) (2011) 235–240, doi:10.1016/j.vibspec.2011.03.002.

2.

Materials Today: Proceedings xxx (xxxx) 1–4

Contents lists available at ScienceDirect

Materials Today: Proceedings

journal homepage: http://ees.elsevier.com

Structural and photoluminescence properties of Er^{3+} doped $SrBi_2Nb_2O_9$ ceramics

Ritushree Shaily, Renuka Bokolia *

Department of Applied Physics, Delhi Technological University, Delhi, India

ARTICLE INFO

Article history:
Received 31 March 2021
Received in revised form 23 May 2021
Accepted 24 May 2021
Available online xxx

Keywords
Photoluminescence
Ferroelectrics
Solid state method
X-Ray diffraction
Orthorhombic distortion
Ceramics

ABSTRACT

In the present study, structural and photoluminescence properties of polycrystalline Er^{3+} doped $SrBi_{2-x}Nb_2Er_xO_9$ (x = 0.00, 0.01, 0.02, 0.03, 0.04, 0.05) ceramics were investigated. All the samples were prepared by the conventional solid-state reaction method and were sintered at 1000 °C for 8 h. X-Ray Diffraction (XRD) confirms the formation of single-phase material with orthorhombic structure. An increase in the lattice parameters and unit cell volume is observed with increasing Erbium (Er^{3+}) content. Strong green emission at 550 nm is seen under 480 nm excitation wavelength at room temperature for an optimum Er content (x = 0.03) and is attributed to $^4S_{3/2} \rightarrow {}^4I_{15/2}$ transitions.

1. Introduction

Photoluminescence (PL), an optical phenomenon is characterized by the emission of two or more photons of the longer wavelength low energy in the visible region means when a molecule absorbs a photon, so one of its electrons gets excited and jumps to the higher electronic excited state and so further the excited electron returns to its lower energy state followed by the emission of photons of lower energy. In rare-earth materials, since different ions have different energy level structure, based on that excitation light sources such as Ultraviolet, Visible, or Infra-red light is chosen. Recently, photoluminescence observed in rare-earth-doped materials has attracted a lot of attention due to its wide range of energy-related applications such as light and displays, temperature sensing, biomedical and solar cells etc. [1,2].

Ferroelectric materials, a type of materials that hold spontaneous polarization and are reversible when subjected to an electric field. Recently, ferroelectric materials have drawn so much attention because of their excellent properties such as high dielectric constant, great fatigue resistance, high Curie temperature, and amazing piezoelectric effects making them attractive materials for different applications such as non-volatile random-access memories (NvRAM), pyroelectric infrared detectors, high capacitance capacitors and optical switches etc. [3,4]. The bismuth layered structure ferroelectric (BLSFs) ceramics, member of Aurivillius family with a chemical formula: $(Bi_2O_2)^{2+}$ $(A_{n-1}B_nO_{3n+1})^{2-}$, where A can be a mono-, di-, or trivalent element (or their combination) with coordination no. 12, for instance Ba^{2+}, Ca^{2+}, La^{3+}, Sm^{3+}, Bi^{3+}, Sr^{2+}, etc., furthermore B is a transition element suited to octahedral coordination possessing coordination no. 6 such as Fe^{3+}, Nb^{5+}, Ti^{3+}, Ta^{5+}, W^{6+},and Mo^{6+}, etc. [5–8], and also, n denotes the number of perovskite layers intermediate between two bismuth oxide layers. Hereabouts, A could be Ca^{2+}, Pb^{2+}, Ba^{2+} and Sr^{2+}, etc. and B perhaps Ti^{4+}, Nb^{5+}, Ta^{5+}, V^{5+}, Mo^{5+}, and W^{6+} etc. Ferroelectric ceramics are very sensitive to compositional modifications such as by changing stoichiometry or even by doping ceramics with numerous elements notably modifying the ferroelectric properties and crystal structure of the ceramics.

$SrBi_2Nb_2O_9$ (SBN), lead-free ferroelectric member of Bismuth Layered Structure Ferroelectric Ceramics belonging to the Aurivillius family (n = 2) has drawn consideration due to their remarkable characteristics such as a high Curie temperature, T_c (718 K), great fatigue resistance, low dielectric loss, reasonable spontaneous polarization, and temperature-insensitive high piezoelectric coefficient and considered for high-temperature applications. Some rare-earth ions like Er^{3+}, Eu^{3+}, Pr^{3+}, etc. [9]. Are widely used as luminescence centres for their potential applications. Thus, by rare-earth doping, the electrical properties and strong luminescence of some ferroelectric materials gets enhanced. In this paper, we report the synthesis of Er^{3+} doped $SrBi_2Nb_2O_9$(SBN) ceramic by conventional solid-state method and study the associated effect of doping of Er^{3+} on their respective crystal structures and luminescence properties.

2. Material synthesis and characterization details

In this experiment, the polycrystalline Er^{3+} doped $SrBi_{2-x}Nb_2Er_xO_9$ (x = 0.00, 0.01, 0.02, 0.03, 0.04, 0.05) ceramics in stoichiometric

* Corresponding author.
E-mail address: renukabokolia@dtu.ac.in (R. Bokolia)

https://doi.org/10.1016/j.matpr.2021.05.520
2214-7853/© 2021.

compositions were synthesized using conventional solid-state reaction method. Firstly, highly purified starting materials Nb_2O_5 (from Aldrich of 99.9% purity), $SrCO_3$ (from Alfa Aesar of 97.5% purity), Bi_2O_3 (from Alfa Aesar of 97.5% purity), and Er_2O_3 (from Alfa Aesar of 97.5% purity) weighed in stoichiometric ratios and then these weighed samples were mixed. After that mixed sample was grinded into a mortar pestle with the addition of ethanol till it gets dried up and repeats the process for 6 h. Then the prepared samples were calcined at 950 °C for 7 h. After calcination, 5 wt% of polyvinyl alcohol (PVA), standard binder is added to the calcined samples and mixed rigorously and then disk-shaped green pellets of all samples were prepared with a diameter of 13 mm and thickness of 1 mm by manual hydraulic press at a pressure of 50 MPa, and keep at rest for 1 min. Hereafter, green pellets of all samples were sintered at 1000 °C for 8 h with intermediate heat treatment at 500 °C for 1 h in order to remove the binder from the pellets [10].

The phase identification and analysis of crystal structure of Er^{3+} doped $SrBi_{2-x}Nb_2Er_xO_9$ were done with the help of the X-Ray diffraction. The XRD spectra achieved by using the Bruker D-8 Advance X-ray diffractometer at Cu-Kα radiation (k_α = 1.5406 Å). The structural morphology and compositional analysis of pure $SrBi_2Nb_2O_9$ and Er^{3+} doped $SrBi_{2-x}Nb_2Er_xO_9$ have been investigated on unpolished sintered pellets by using the JEOL 661 Scanning electron microscopy (SEM) equipped with Amkette energy dispersive spectrometer (EDS). The photoluminescence (PL) spectra of Er^{3+} doped SBN recorded at an excitation wavelength, λ_{ex} = 480 nm.

3. Results and discussion

3.1. Structural analysis

Erbium, rare earth metal belongs to the lanthanide series shows most stable + 3 oxidation state thus it is easy to substitute Er^{+3} in a place of Bi^{+3} [11]. Fig. 1, shows XRD spectra of pure $SrBi_2Nb_2O_9$ and Er^{3+} doped $SrBi_{2-x}Nb_2Er_xO_9$ ceramic powders at varying Er^{3+} concentrations (x = 0.00, 0.01, 0.02, 0.03, 0.04, 0.05). From the XRD analysis in the range 2θ = 10–80, the observed Bragg's reflection was indexed and found closely matching with the standard diffraction pattern data of $SrBi2Nb_2O_9$ with JCPDS card#01–089- 8154 and confirmed the formation of single phase with no traces of secondary phases or unreacted phases present, specifying that Er^{3+} ions completely dissolved in SBN host lattice without any significant structural change of the host lattice. Thus, all samples crystallized in the orthorhombic phase, associated with the space group $A2_1am$. Also, the highest diffraction peak associated with (1 1 5) plane of $SrBi_2Nb_2O_9$ was detected for all concentrations conforming to the bismuth layered structure with n = 2 and the results are in agreement with the earlier reports indicating the strongest diffraction corresponding to (112n + 1) reflection in the Aurivillius phase for BLSF compositions. The lattice parameters were calculated with the help of PowderX software, and the structural parameters tabulated in Table 1.

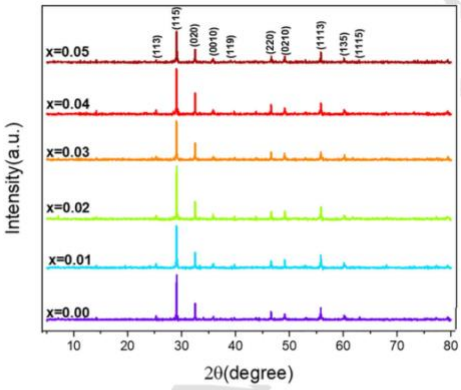

Fig. 1. The XRD patterns of pure and Er^{3+} doped $SrBi_2Nb_2O_9$ at different concentrations of Er^{3+} based on the formula $SrBi_{2-x}Nb_2Er_xO_9$ ceramics.

It is noted from the Fig. 2. with an increase in the concentration of Er3 + ions the XRD peaks at 29.08 shifted towards lower 2θ values shows that the Er3 + ions completely diffused into the host lattice along with the increase in lattice parameters which is due to the difference in ionic radii of Bi3+(r = 102A) and Er3+ (r = 0.88A) leading to structural distortion and is well supported with the increasing elemental ratio of (Er/Bi) as seen through EDS compositional analysis (Table 2). Also, with the increase in the concentration of erbium ions there is an expansion in a volume of unit cell, an increase in the orthorhombic distortion and orthorhombicity followed by the increase in tetragonal strain. [3,9].

The microstructure of the sintered ceramic surface of $SrBi_{2-x}Nb_2Er_xO_9$ is shown in Fig. 3. The morphological details reveal the formation of randomly oriented grains of varying size with a presence of porosity in the microstructure as solid-state method leads to more pores and non-uniform grain size, and was achieved under prepared condition. The micrographs indicated insignificant changes in grain size with varying increasing Er content. The compositional analysis of pure $SrBi_2Nb_2O_9$ and Er3 + doped $SrBi_{2-x}Nb_2Er_xO_9$ pellets was done by EDS (Energy Dispersive Spectrum) and the data of the elements were given in the Table 2.

3.2. Photoluminescence spectra

The photoluminescence (PL) properties of Er^{3+} doped $SrBi_{2-x}Nb_2Er_xO_9$ (x = 0.00, 0.01, 0.02, 0.03, 0.04 and 0.05) ceramics for different concentrations were examined under the excitation wavelength, λ_{ex} = 480 nm at room temperature and acquired photoluminescence emission spectrum is shown in Fig. 4. From the observations, all the Er doped $SrBi_{2-x}Nb_2Er_xO_9$ ceramics display strong green emission ranging from 529.2 nm to 549.8 nm, (centred at 529.2 nm, 540.96 nm, 542.95 nm, and 549.8 nm) refers $^2H_{11/2}\rightarrow{}^4I_{15/2}$, and $^4S_{3/2}\rightarrow{}^4I_{15/2}$ transitions, respectively and light greenish emission was observed at

Table 1
Lattice parameters of $SrBi_{2-x}Nb_2Er_xO_9$.

$SrBi_{2-x}Nb_2Er_xO_9$	a(Å)	b(Å)	c(Å)	Volume (Å^3)	Orthorhombic Distortion, b/a	Orthorhombicity, 2(a-b)/(a + b)	Tetragonal strain, c/a
x = 0.00	5.4933	5.5136	25.035	758.2565	1.003695	0.00369	4.55737
x = 0.01	5.4938	5.5141	25.039	758.5155	1.003695	0.00369	4.557683
x = 0.02	5.4943	5.5146	25.043	758.7745	1.003695	0.00369	4.557996
x = 0.03	5.4946	5.5152	25.047	759.0197	1.003749	0.00374	4.558476
x = 0.04	5.4949	5.5157	25.051	759.2512	1.003785	0.00378	4.558955
x = 0.05	5.4951	5.5162	25.055	759.4689	1.003840	0.00383	4.559517

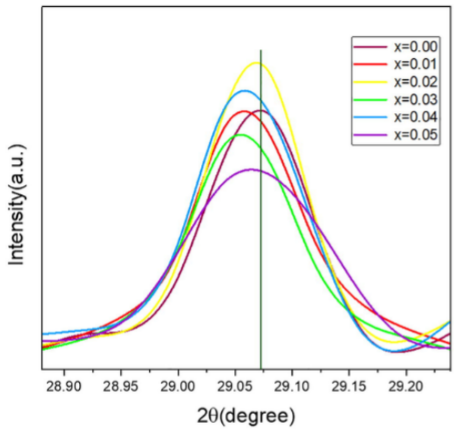

Fig. 2. Shift of strongest XRD peaks (1 1 5) at different Erbium concentrations.

Table 2
EDS compositional analysis.

Nominal composition	Sr (at%)	Bi (at%)	Nb (at%)	Er (at%)	Er/Bi
Stoichiometric $SrBi_2Nb_2O_9$	5.731	11.797	12.691	–	–
Present Work $SrBi_{2-x}Nb_2Er_xO_9$ x					
0.00	3.53	11.151	6.363	–	–
0.01	2.652	8.328	4.775	0.034	0.004
0.02	2.653	8.319	4.777	0.068	0.008
0.03	2.654	8.253	4.779	0.103	0.012
0.04	2.656	8.215	4.782	0.137	0.016
0.05	2.657	8.177	4.784	0.172	0.021

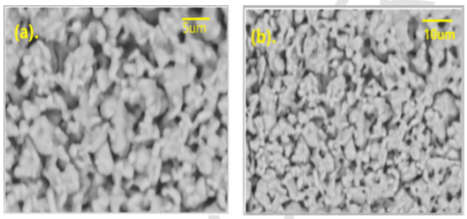

Fig. 3. Surface morphology of SBN ceramic.

579.4 nm. Furthermore, the splitting of PL spectra ranging from 540.96 nm to 549.8 nm into several components is due to Stark effect (or Stark splitting) [12,13]. The highest peak of PL emission spectra monitored at a wavelength of 549.8 nm i.e., the strong green emission refers to the excitation of Er3 + ions from ground level $^4I_{15/2}$ to higher energy level $^4S_{3/2}$ rather than the host material. With an increase in the doping content of Er3 + firstly, the PL intensity increases up to × = 0.03 and then decreases because by means of concentration quenching while the position of emission peaks for all remains the same. As indicated in PL spectra, the maximum emission intensity occurs at a concentration, x = 0.03. So, Er3 + doped $SrBi_{2-x}Nb_2Er_xO_9$

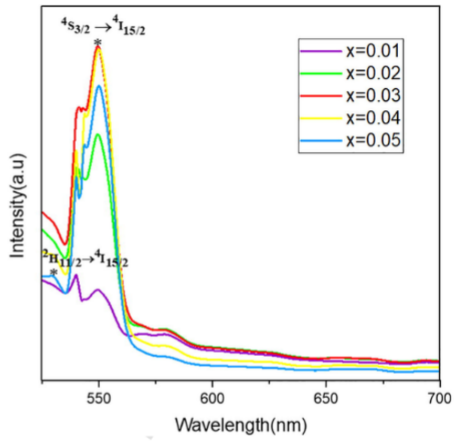

Fig. 4. PL spectra of Er^{3+} doped $SrBi_{2-x}Nb_2Er_xO_9$ at different concentrations under 480 nm excitation wavelength.

(x = 0.00, 0.01, 0.02, 0.03, 0.04 and 0.05) ceramics can be considered as appropriate visible light excited green phosphors where Er3 + doped $SrBi_{2-x}Nb_2Er_xO_9$ with concentration, x = 0.03 ceramics outshines others [14–16].

4. Conclusion

The synthesis of Er^{3+} doped $SrBi_2Nb_2O_9$ ceramics, their structural analysis and PL properties were investigated and studied. The study of XRD patterns of pure SBN and Er^{3+} doped SBN indicates that the pure SBN is orthorhombic in nature with no secondary phases and with further increase in the doping concentration of Er^{3+} ion in SBN results in the shifting of strongest peak (1 1 5) towards lower angles and there is an increase in orthorhombic distortion and orthorhombicity with the increase in Er content. The PL properties implies, at a 480 nm excitation wavelength, strong green emission bands observed at 549.8 nm and strongest emission intensity was achieved at a concentration of Er^{3+} when x = 0.03.

CRediT authorship contribution statement

Ritushree Shaily: Conceptualization, Data curation, Investigation, Methodology, Writing - original draft. **Renuka Bokolia:** Conceptualization, Methodology, Supervision, Writing - original draft, Writing - review & editing.

Declaration of Competing Interest

The authors declare that they have no known competing financial interests or personal relationships that could have appeared to influence the work reported in this paper.

Acknowledgements

Authors would like to express gratitude towards Research Project Grant (F.NO. DTU/IRD/619/2019/2112), Delhi Technological University for granting research facilities. Authors wish to acknowledge the help provided by the technical and support staff in the Department of Applied Physics, Delhi Technological University for aiding with the characterization of samples.

References

[1] Y. Zhao, X. Wang, Y. Zhang, Y. Li, X. Yao, Optical temperature sensing of up-conversion luminescent materials: Fundamentals and progress, J. Alloy. Compd. 817 (2020) 152691, doi:10.1016/j.jallcom.2019.152691.

[2] D.P. Volanti, I.L.V. Rosa, E.C. Paris, C.A. Paskocimas, P.S. Pizani, J.A. Varela, E. Longo, The role of the Eu3+ ions in structure and photoluminescence properties of SrBi2Nb2O9 powders, Opt. Mater. (Amst) 31 (6) (2009) 995–999, doi:10.1016/j.optmat.2008.11.006.

[3] T. Wei, et al., Enhanced up-conversion photoluminescence and dielectric properties of Er- and Zr-codoped strontium bismuth niobate ceramics, Ceram. Int. 41 (9) (2015) 12364–12370, doi:10.1016/j.ceramint.2015.06.067.

[4] D. Peng, H. Sun, X. Wang, J. Zhang, M. Tang, X. Yao, Red emission in Pr doped CaBi4Ti4O15 ferroelectric ceramics, Mater. Sci. Eng. B Solid-State Mater. Adv. Technol. 176 (18) (2011) 1513–1516, doi:10.1016/j.mseb.2011.09.009.

[5] V. Senthil, T. Badapanda, A. Chandra Bose, S. Panigrahi, Enhancement of dielectric and ferroelectric properties of dysprosium substituted SrBi2Ta2O9 ceramics, J. Mater. Sci. Mater. Electron. 27 (2) (2016) 1602–1608, doi:10.1007/s10854-015-3930-2.

[6] S. Jain, P. Ganguly, S. Devi, A.K. Jha, Structural, dielectric and ferroelectric studies of molybdenum substituted Sr2Bi2Nb2O9 ferroelectric ceramics, Ferroelectrics 381 (1) (2009) 152–159, doi:10.1080/00150190902870051.

[7] O. Jalled, Z. Alharbi, S.R. Alharbi, A. Saeed, M. Alhassan, S. Al-Heniti, H.Y. Mohammed, Y. Al-Hadeethi, F. Al-Marzouki, A. Al-Mujtaba, Synthesis and dielectric properties of nanocrystalline strontium bismuth niobate, J. Nanosci. Nanotechnol. 17 (1) (2017) 594–600, doi:10.1166/jnn.2017.12459.

[8] L. Yu, J. Hao, Z. Xu, W. Li, R. Chu, G. Li, Strong photoluminescence and good electrical properties in Eu-modified SrBi2Nb2O9 multifunctional ceramics, Ceram. Int. 42 (13) (2016) 14849–14854, doi:10.1016/j.ceramint.2016.06.119.

[9] T. Wei, C.Z. Zhao, Q.J. Zhou, Z.P. Li, Y.Q. Wang, L.S. Zhang, Bright green upconversion emission and enhanced ferroelectric polarization in Sr1-1.5xErxBi2Nb 2O9, Opt. Mater. (Amst) 36 (7) (2014) 1209–1212, doi:10.1016/j.optmat.2014.03.001.

[10] A. Banwal, R. Bokolia, Phase evolution and microstructure of BaBi2Nb2O9 ferroelectric ceramics, Mater. Today Proc. 3, xxxx (2020) 2–5, doi:10.1016/j.matpr.2020.09.380.

[11] P. Henderson, "Rare earth element geochemistry, Developments in geochemistry," vol. 2, p. 510, 1984, [Online]. Available: http://ezproxy.lib.utexas.edu/login?url=http://search.ebscohost.com/login.aspx?direct=true&db=geh&AN=1984-023694&site=ehost-live.

[12] A. Tomar, M. Singh, S. Singh, L. Sharma, S. Arya, S. Kasana, Ultraviolet Quantum Cutting through down Conversion Luminescence Behaviour of Er3+ Substituted Sr0.7Bi2.2Nb2O9 (BLFS) Ceramics, Integr. Ferroelectr. 204 (1) (2020) 33–37, doi:10.1080/10584587.2019.1674983.

[13] T. Honma, T. Komatsu, D. Zhao, H. Jain, Writing of rare-earth ion doped lithium niobate line patterns in glass by laser scanning, IOP Conf. Ser. Mater. Sci. Eng. 1 (2009) 012006, doi:10.1088/1757-8981/1/1/012006.

[14] L. Mukhopadhyay, V.K. Rai, R. Bokolia, K. Sreenivas, 980 nm excited Er3+/Yb3+/Li+/Ba2+: NaZnPO4 upconverting phosphors in optical thermometry, J. Lumin. 187 (October) (2017) 368–377, doi:10.1016/j.jlumin.2017.03.035.

[15] R. Bokolia, O.P. Thakur, V.K. Rai, S.K. Sharma, K. Sreenivas, Dielectric, ferroelectric and photoluminescence properties of Er3+ doped Bi4Ti3O12 ferroelectric ceramics, Ceram. Int. 41 (4) (2015) 6055–6066, doi:10.1016/j.ceramint.2015.01.062.

[16] R. Bokolia, V.K. Rai, L. Chauhan, K. Sreenivas, Structural and light up-conversion luminescence properties of Er3+-Yb3+-W6+ substituted Bi4Ti3O12, AIP Conf. Proc. 1731 (2016) 4–7, doi:10.1063/1.4948208.